Desalination 613 (2025) 119083

Contents lists available at ScienceDirect

Desalination

journal homepage: www.elsevier.com/locate/desal

Recovery of uranium from seawaters by ultra/nano filtration assisted by complexation

C. Xing [a,b], B. Bernicot [b], S. Monge [c], V. Darcos [d], G. Arrachart [b,*], S. Pellet-Rostaing [b,**]

[a] Department of Aquatic Sciences and Assessment, Swedish University of Agricultural Sciences, Uppsala, Sweden
[b] ICSM, Univ Montpellier, CEA, ENSCM, CNRS, Marcoule, France
[c] ICGM, Univ Montpellier, CNRS, ENSCM, Montpellier, France
[d] IBMM, Univ Montpellier, CNRS, ENSCM, Montpellier, France

HIGHLIGHTS

- UF/NF assisted by complexation sterically reject UO_2^{2+} in 35 g L^{-1} seawater.
- The best performance achieves ~96 % U rejection vs <5 % $Na^+/K^+/Ca^{2+}/Mg^{2+}$ rejection.
- *N*-acryloylalendronate polymers show high uranium uptake and sodium separation.
- Uranium is released from polymers using acid treatment without membrane damage.

GRAPHICAL ABSTRACT

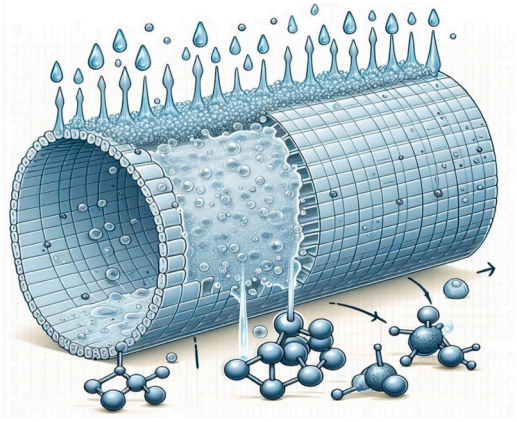

ARTICLE INFO

Keywords:
Uranium
Separation
Seawater
Inorganic membrane
Ultra/nano filtration assisted by complexation
Hydrophilic polymer

ABSTRACT

Uranium extraction from unconventional sources such as seawater is an important complementary source for nuclear fuel production. A common method for separating ions in aqueous solutions is ultra/nano filtration (UF/NF), which employs both electrical and steric effects. While commercial inorganic UF/NF membranes have been used to separate uranium from other salts in natural or synthetic seawater, the high ionic strength of seawater tends to reduce the electrical effect. To overcome this, hydrophilic polymers with high selectivity towards uranium have been introduced into seawater to assist the filtration by complexation. This allows uranium to be rejected by the steric effect while allowing other metal ions to pass through the membrane. The performance of different hydrophilic polymers containing complexing functional groups, including alendronic acid, bis(phosphonic acid), and catechol, was evaluated to assist in the filtration process to separate uranium from other competitive metal ions (Na, K, Ca, Mg). The results show that two hydrophilic polymers, based on *N*-acryloylalendronate, demonstrate the best performance for the separation of uranium, achieving a sorption capacity

* Corresponding author.
** Correspondence to: G. Arrachart and S. Pellet-Rostaing, ICSM, Univ Montpellier, CEA, ENSCM, CNRS, Marcoule, France.
E-mail addresses: guilhem.arrachart@umontpellier.fr (G. Arrachart), stephane.pellet-roasting@cea.fr (S. Pellet-Rostaing).

https://doi.org/10.1016/j.desal.2025.119083
Received 23 March 2025; Received in revised form 20 May 2025; Accepted 30 May 2025
Available online 31 May 2025

of over 200 mg U/g polymer and an extremely high separation factor of U to salts ($SF_{(U/Na)} > 6000$ for a (poly (NAM-*co*-ALNAm)). By using filtration assisted by complexation with polymers, uranium can be effectively rejected while maintaining low rejections for other salts in high salinity seawater of at 35 g L^{-1}. Uranium can be released from the complex by spiking the seawater by concentrated nitric acid or sulfuric acid. These laboratory-scale filtration experiments have significant industrial applications for the recovery uranium from seawater.

1. Introduction

The extraction of uranium is one of the seven chemical separations that will change the world [1]. It is found in trace amounts everywhere, including in seawater. The surface and underground uranium will be exhausted sooner or later as the human demand for uranium increases. Historically, conventional mines have been the main source of uranium, more than half of the world's uranium mines are mined using in-situ leaching process [2]. However, most of the world's reserves are unconventional resources and are unusable under current economic conditions [3]. 71 % of the Earth's surface is covered by oceans and seas, including 137,109 km^3 of water. There are approximately 50 quadrillion tons of minerals and metals dissolved in all the world's seas and oceans [4]. Seawater contains about 3.3 mg of uranium per cubic meter, i.e., 4.5 billion tons of uranium are dissolved in the oceans [5], which is a much larger amount compared to the land and underground resources [6]. These nearly limitless reserves provide a substantial potential source of nuclear fuel despite the challenges and difficulties to be overcome [4,6–8]. Uranium forms highly stable Ca-UO_2-CO_3 and Mg-UO_2-CO_3 species in seawater [9,10]. Efficient and selective extraction of uranium from seawater is particularly challenging due to the complex solution chemistry in seawater, including high salt concentration (average salinity around 35 g L^{-1} mainly due to NaCl), high carbonate concentration, basic pH (7.5–8.5), temperature (5–35 °C), low uranium concentration (~3.3 μg L^{-1}), and other metal ions at similar or higher concentrations.

The recovery of uranium from seawater has been a hot topic in recent years, numerous materials have been investigated to achieve the concentration of uranium from seawater in nearly 7 decades [7,11–13], amidoxime-based adsorbents are currently considered the most promising [7,14–24] due to their special affinity for uranium [25–27]. Conventional extraction methods are based on the distribution of two phases [5,11,28]. These two-phase distribution processes, which include an aqueous metal ion solution and a water-insoluble polymer/resin, have disadvantages such as long contact times. These heterogeneous systems can be avoided by using separation methods based on membrane processes in the aqueous homogeneous phase, which are among the most promising techniques for the enrichment of various species from water [29–31]. Membrane separation includes microfiltration (MF), ultrafiltration (UF), nanofiltration (NF), and reverse osmosis (RO), etc. UF/NF has been evaluated for recovery of valuable metals from urban mines [32,33], seawater desalination brine [34], and industrial wastewater [35]. It has been applied in selective removal of minor actinides from lanthanides [36–41], removal of uranium from drinking water [42] and from seawater [43], separation of uranium from other metal ions from fresh and salt water [44]. Besides, renewable energy driven membrane technologies have been investigated for water treatment and ion separation [45–48].

The UF/NF process can concentrate multivalent metal ions by rejection attributed to a combination of various mechanisms including steric, electrical, Donnan, dielectric and transport effects [49]. Steric effect and electrical effect are two major factors influencing the rejection. Charged species in solution can be rejected by electrical exclusion when they encounter electrical interactions with charges in the membrane material. Meanwhile, the membrane will retain species with molecular weights higher than its cut-off, while small molecules such as solvents and micro solutes will freely pass through it [50]. If the target component is not charged with a molar mass smaller than the membrane molecular weight cut-off (MWCO), it cannot be rejected by either the steric effect or the electrical effect. Hydrophilic complexing agents, capable of complexing the target ions, are added to the solution, to change the charge and/or the size of the species to obtain a metal-polymer complex of sufficient molecular size (larger than MWCO) to be retained by steric effect, while the non-complexed ions pass through. This combination of the membrane process and polymer complexation processes is referred as filtration assisted by complexation process. This technique, developed by the laboratory of Geckeler et al. [51], is based on the separation of ions bound to hydrophilic polymers with chelating groups from non-complexed ions/unbound metals [51]. The major advantage of this technique is the homogeneous nature of the separation. Thus, it largely avoids the phenomenon of mass transfer, or diffusion, which is limiting in heterogeneous methods [52]. Many soluble and hydrophilic polymers have been found to be suitable for the separation and enrichment of metal ions in association with membrane filtration [53]. The concept of complexation-assisted filtration has been applied in several industrial fields, including the water treatment [54–57], the depollution of aqueous solutions [50,58,59], the separation of monovalent cation with hydrophilic macrocycles [60,61], separation of the divalent metals with EDTA, NTA, citric acid [62], with polyamino carboxylate ligands [39], with chitosan [63], removal of heavy metals from wastewaters using the water-soluble amine and imine polymers [52,53,55,56,59,64–68]. According to an early research study of Geckeler et al. [69], some polymers, such as poly(iminoacetic acid) (PIAA), sulfonated oxyquinoline derivative of poly-(ethylenimine) SOPEI, poly (acrylic acid) (PAA), poly(urethane) (PU), poly(vinyl alcohol) (PVAL), phosphorylated derivative of poly(vinyl alcohol) (PPVAL), poly(ethylenimine) (PEI), modified poly(ethylenimine) (PEI-SN), poly(diallyl dimethyl ammonium chloride) (DADMAC), etc., have been demonstrated to form complexes with U(VI). Dipicolinic acid (DPA) is known for its ability to extract metals, particularly actinides (VI) (U, Np, Pu, Am) with the formation of mononuclear trimeric complexes (metal / ligand ratio 1:1 and 1:2) [70]. According to the research of Brown et al. [71], diethylenetriaminepentaacetic acid (DTPA) can form a strong complex with U(IV) [72]. Antonina et al. [73] have studied the removal of uranium from synthetic water contaminated with UO_2SO_4 and with dissolved CO_2 by ultrafiltration combinated with complexation. PEI with the molecular mass of 60,000 g mol^{-1} was used as the complexing agent. The rejection of U(VI) reached 91–95 % at pH 9.0 when no polyelectrolytes were present. When polyethylenimine was used in a concentration ratio of C(PEI)/C(U) = 4:1, the rejection reached 99.9 % using a UPM-20 polyamide membrane in the pH range of 5–9. Pascal et al. [74] worked on micellar-enhanced ultrafiltration (MEUF) for the uranyl ion removal with the sodium alkylsulfate micelles and the polysulfone UF membrane. They found that the uranyl ion is rejected by the UF membrane due to the strong interaction of the ion with the micellar surface. Despite this research on uranium separation from water, there is no research on uranium uptake by UF/NF assisted by complexation from seawater.

Although alternative membrane-based approaches have been explored for uranium separation, each suffers from significant drawbacks when applied to high-salinity seawater. For instance, polyethylene imine (PEI) and its phosphorylated derivatives form robust U(VI) complexes; however, their broad cation affinity results in poor selectivity over Na^+, Ca^{2+}, and Mg^{2+}. Additionally, the high ionic strength of seawater severely screens their electrostatic rejection mechanism [23,75]. DTPA and EDTA ligands effectively chelate UO_2^{2+} in low-

salinity systems, but their small metal–ligand complex sizes often fall below typical UF/NF MWCOs, necessitating tight membranes that rapidly foul and exhibit limited acid stability during regeneration [76,77]. Micellar-enhanced ultrafiltration with sodium dodecyl sulfate (SDS) can increase U rejection via surfactant–uranyl interactions. However, the need to recover the surfactant and the micelles' sensitivity to salinity and pH fluctuations make continuous, industrial-scale operation difficult [78]. Chitosan-based systems offer biodegradable platforms for metal binding; however, they too exhibit low selectivity in seawater and are susceptible to swelling and shrinking cycles that degrade membrane integrity with repeated use [79]. Recently, we reported the application of inorganic UF/NF membranes for the separation of uranium from saline water. However, the use of inorganic UF/NF membranes does not allow the effective separation or concentration of uranium from seawater (35 g L^{-1}), mainly due to a very high ionic strength and to the formation of neutral mixed complexes of uranium with calcium, magnesium, and carbonates, which inhibits rejection by electrical effect [44]. Therefore, the complexation assisted filtration process has been proposed to overcome this problem. This process relies on the steric effect to achieve high rejection of uranium, separating and concentrating U from seawater. As shown in the Fig. 1, the size of the uranium can be artificially increased and/or the charge of the species can be changed by introducing hydrophilic polymers with a high affinity for uranium. This allows for the rejection of uranium by steric exclusion. Consequently, the uranium-polymer complex, which has a molar mass higher than the MWCO is rejected by the membrane. The artificially enlarged uranium cannot pass through the membrane. Meanwhile, other metal cations that are not complexed with the polymer pass through the membrane without any constraint. These limitations—nonselective binding, low complex size, membrane fouling, and poor acid resilience—collectively underscore the need for high-affinity, steric-based complexation strategies. Such strategies include phosphonate-functionalized polymers with affinity for uranium, which overcome ionic screening and enable robust UF/NF performance in marine environments.

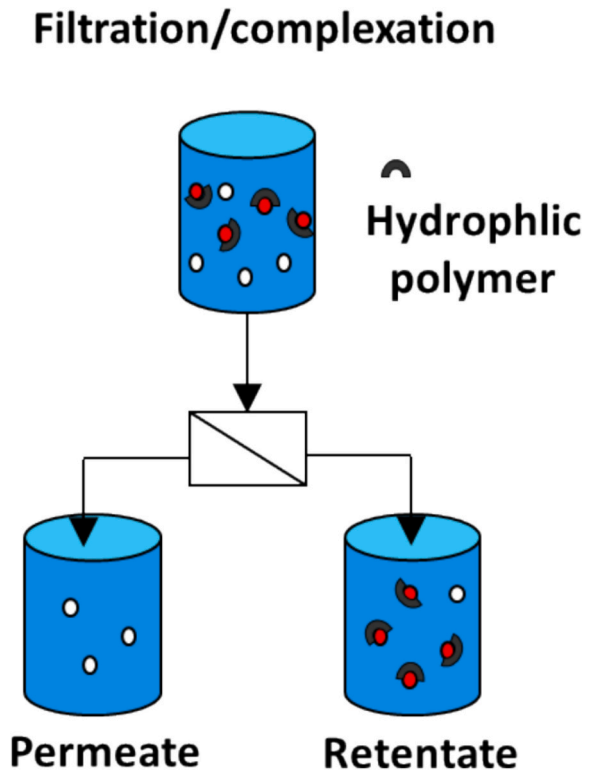

Fig. 1. Schematic representation of ultra/nanofiltration complexation.

The present work investigates the separation and concentration of uranium (VI) in seawater from monovalent and divalent cations by ultra/nanofiltration assisted by complexation Six commercial or synthetized hydrophilic polymers bearing phosphoric acid or phosphonate functionalities (e.g., alendronate-based polymers, poly(ethylene glycol), α-methoxy, ω-catechol, and poly(ethylene glycol), α,ω-bis(phosphonic acid)) were evaluated for their ability to form high-molecular-weight U–polymer complexes that are sterically retained by membranes. For each polymer, the rejection kinetics and the separation factor of U to other metals under seawater conditions were determined. The sorption capacity of these polymers to U was estimated. Finally, the desorption of U from the loaded polymer complex was realized using acidic solutions. These data were integrated into a process flow sheet for scalable uranium recovery from seawater.

2. Experiments

2.1. Materials and methods

Ultra/nano filtration experiments are investigated in a 1 L volumetric reactor filled with U-doped seawater mixed with hydrophilic polymer. The experiments are performed with a SIVA laboratory-scale membrane system which is illustrated in Fig. S.1 with a detailed caption.

2.2. Analytical procedure

ICP-OES (Inductively Coupled Plasma Optical Emission Spectroscopy, iCAP 7000 Series) with a standard deviation of ±2 % was used for the quantification of U, Na, Ca, Mg, K in solution.

2.3. Filtration experiments

The rejection of metal ions is evaluated from the retentate and permeate concentration of the samples collected during the experiments. The rejection Ri (%) of a substance i is calculated with the following Eq. (1):

$$R_i(\%) = 100 \times \left(1 - \frac{C_p^i}{C_{Ret}^i}\right) \quad (1)$$

where C_{Ret}^i is the concentration of i in the retentate (flux that has not passed through the pores of the membrane) and C_p^i is the concentration of i in the permeate (corresponding to the flux that has passed through the pores of the membrane). The concentration of retentate can be considered equal to the feed concentration because the flux rate of retentate is far higher than that of permeate.

After each filtration experiment, the filtration system is first washed with a basic NaOH solution (10 mL of 2 M NaOH solution in 1 L of distilled water). After this first wash, the system is washed several times with distilled water until the pH reaches the pH value of distilled water. The system is then washed with nitric acid (200 µL of HNO_3 67–69 % concentrated in 1 L of distilled water) and washed with distilled water until the pH is the same as the distilled water for the next experiment.

2.4. Membrane

The inorganic filtration membrane used was a multilayer structure with a TiO_2/ZrO_2 active layer and a tubular channel titanium support (CéRAM™ - TAMIS INDUSTRIES, Nyons, 26 - France). The filtration layer is based on a tubular titanium support with a length of 25 cm and an outer diameter of 10 mm. Monocanal membranes with a hydrodynamic diameter of 6 mm are used, allowing the passage of the fluid within the hollow part. These multilayer membranes employed are specified by the manufacturer to withstand pH 0–14 without structural damage or pore-size alteration. The MWCO used for the membrane was either 1 kDa or 5 kDa, depending on the hydrophilic polymer used.

2.5. Sample preparation

2.5.1. Aqueous solutions

The composition of the solutions under investigation is shown in the Table S.3. The UF/NF process assisted by complexation was used to evaluate Mediterranean seawater doped with U at concentrations ranging from 2 to 175 mg L^{-1}. Additionally, a solution of U, NaCl, and $NaHCO_3$ (solution 1), which has a similar salinity to that of Mediterranean seawater (35 g L^{-1}), was used for the experiments. Uranium was doped with the mother solution of UO_2^{2+} at 1 g L^{-1} at pH 10, diluted from 10 g L^{-1} uranyl nitrate $UO_2(NO)_3{\cdot}6H_2O$, in HNO_3 2 %. The pH was controlled by adding pure NaOH powder into the solution. Analytical grade of NaCl, $MgCl_2$, $CaCl_2$, KCl, Na_2SO_4, $NaHCO_3$ salts were used for the preparation of synthetic seawater. The pH value of the filtration feed was measured with a pH meter (Metrohm 781 pH meter) and adjusted to 8.2–8.3 by adding 2 M NaOH or 1 M HCl. Concentrated nitric acid 67–69 % or sulfuric acid 96–98 % was used for desorption experiments.

2.5.2. Hydrophilic polymers

Various hydrophilic polymers have been investigated for the uranium chelation and the application in the ultra/nanofiltration assisted by complexation.

A first series consists of synthesized hydrophilic polymers (Fig. 2(a)) comprising an acryloyl repeating unit functionalized by an alendronate group, *N*-acryloylalendronate (ALNAm), which repeating unit is associated with a hydrophilic block of *N*-acryloylmorpholine (NAM), (poly(NAM-*co*-ALNAm)) **I** or double hydrophilic diblock copolymers of *N*-acryloylmorpholine (NAM) and *N*-isopropylacrylamide (NIPAAm), (poly(NIPAAM)-b-poly(NAM-*co*-ALNAm)) **II** with different degrees of polymerization were studied (Table S.4). The polymers were prepared via a combination of RAFT polymerization and post-polymerization modification as reported by Darcos et al. [80]. The molecular weights were determined by size exclusion chromatography (SEC), which highlighted monomodal profiles with narrow molecular weight distributions. These distributions were in good agreement with the theoretical values, indicating good control over the polymerization process.

A second series consisting of commercial poly(ethylene glycol) PEG-based polymers available from Specific Polymers® were studied: i) a poly(ethylene glycol), α,ω-bis(phosphonic acid), (**III** PEG-bis (phosphonic acid)) and a poly(ethylene glycol), ii) α-methoxy, ω-catechol, (**IV** PEG-catechol), Fig. 2(b) and (c), respectively.

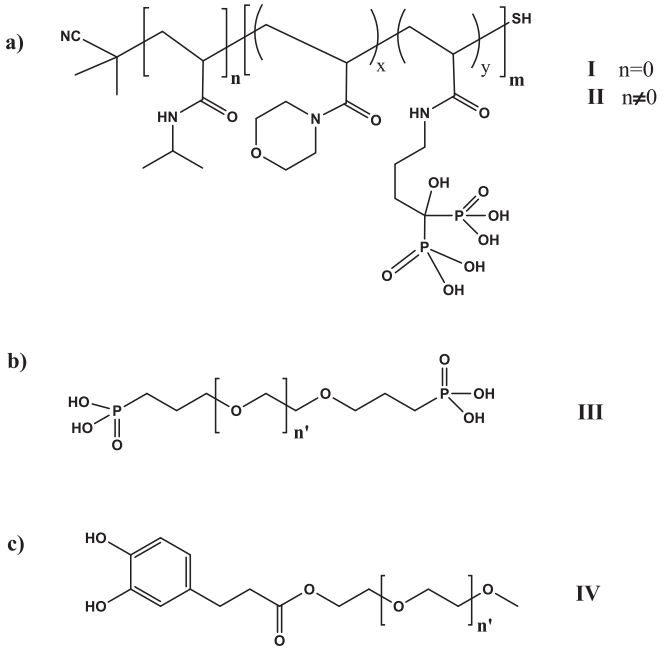

Fig. 2. General structure of the hydrophilic polymers used in this study: (a) (poly(NAM-*co*-ALNAm)) $n = 0$ **I** and (poly(NIPAAM)-b-poly(NAM-*co*-ALNAm)) $n \neq 0$ **II**; (b) (PEG-bis(phosphonic acid)) **III**; (c) (PEG-catechol) **IV.**

2.6. Evaluation of polymer sorption capacity by membrane filtration

2.6.1. Rejection kinetics

The rejection kinetics of filtration assisted by complexation with polymer towards uranium is evaluated by filtration experiments under seawater conditions. A hydrophilic polymer with specific functions, allowing an effective complexation of uranium, is added to the already prepared U-doped seawater. Depending on the studies performed, the amount of hydrophilic polymer was varied. After stirring and complete solubilization, this solution is engaged into the filtration tank to carry out the complexation filtration experiment with the filtration system shown in Fig. S.2.

Throughout the process, the retentate and the permeate are returned to the feed, maintaining an almost constant volume. The recovery of the permeate and retentate, both approximately 10 mL, is performed approximately every 30 min to evaluate the rejection of each metal ion by ICP-OES measurement. The experiments were repeated several times to improve the reliability of the results.

2.6.2. Sorption capacity

The sorption capacity of the hydrophilic polymer for uranium was estimated by fixing the concentration of the polymer while varying the uranium concentration, the schematic diagram is shown in the Fig. S.3. To determine the sorption capacity, the filtration was conducted with 1 L of seawater doped with U at an initial concentration of C_0, and containing the hydrophilic polymer. The permeate and retentate were collected after 2 h. A calculated amount of U was then added to the filtration tank, 2 M NaOH or 1 M HCl was used for maintaining the pH at 8.2–8.3. After another 2 h, the permeate and retentate were collected. The same procedure was repeated until the U concentration in the feed reached C_f. The conditions for the filtration assisted by the complexation experiments are shown in the Table 1. For polymer **I-B**, two series were tested on a 5 kDa membrane: a high-loading series with [U] = 20–75 mg L^{-1} at 1 g L^{-1} polymer, and a low-loading series with [U] = 2–50 mg L^{-1} at 0.06 g L^{-1}. Polymer **II-A** was evaluated at [U] = 20–75 mg L^{-1} with 0.5 g L^{-1} polymer on 5 kDa, while **II-B** underwent three series on the same membrane: a low-loading run ([U] = 2–50 mg L^{-1}, 0.06 g L^{-1} polymer), an intermediate-loading run ([U] = 20–75 mg L^{-1}, 0.08 g L^{-1}), and a high-loading run ([U] = 20–175 mg L^{-1}, 1 g L^{-1}). For the polymers **III** and **IV**, 1 kDa membrane was used. Polymer **III** was tested

Table 1
Conditions of filtration assisted by complexation experiments.

Hydrophilic polymer	[U] (mg L^{-1})	[Polymer] (g L^{-1})	Membrane
Conditions of filtrations in rejection kinetics study			
I-A	20	1	5 kDa
I-B	20	1	5 kDa
II-A	20	1	5 kDa
II-B	2	0.1	5 kDa
III	20	2	1 kDa
IV	20	2	1 kDa
Conditions of filtrations in sorption capacity study			
I-B	20–75	1	5 kDa
I-B	2–50	0.06	5 kDa
II-A	20–75	0.5	5 kDa
II-B	2–50	0.06	5 kDa
II-B	20–75	0.08	5 kDa
II-B	20–175	1	5 kDa
III	2–50	0.1	1 kDa
III	2–50	0.5	1 kDa
III	20–75	1	1 kDa
IV	20–75	1	1 kDa

at [U] = 2–50 mg L^{-1} with polymer dosages of 0.1, 0.5, and 1 g L^{-1} (the latter covering [U] = 20–75 mg L^{-1}), whereas polymer **IV** was evaluated at [U] = 20–75 mg L^{-1} and 1 g L^{-1} polymer. **I-A** was not tested due to its low affinity for U observed in previous kinetics studies.

2.6.3. Desorption

After the filtration experiments, a small amount of concentrated nitric acid 67–69 % or sulfuric acid 96–98 % was spiked into the seawater retentate, then the filtration was conducted with the retentate in closed cycle to evaluate the desorption of U from the U–polymer complexes in acidic environments. Spiking with concentrated strong acid was performed without damaging the membrane, as inorganic membranes can withstand pH extremes ranging from 0 to 14. The recovery of the permeate and retentate was performed after 2 h of filtration. The schematic presentation is shown in Fig. S.4.

To obtain the best desorption of U, the following experiments were performed:

(a) retentates with different polymers were doped with concentrated nitric acid to estimate the desorption of U by HNO_3 at 0.1 mol L^{-1};
(b) retentates with **I-B** were doped with different amounts of concentrated nitric acid to estimate the effect of nitric acid concentration on the desorption;
(c) retentates with different polymers were doped with different amount of concentrated nitric acid to estimate the effect of nitric acid concentration on the desorption;
(d) retentates with different polymers were doped with different amount of concentrated sulfuric acid to estimate the effect of sulfuric acid concentration on the desorption.

The experimental desorption conditions are shown in Table S.6.

3. Results and discussion

3.1. Hydrophilic polymer selection

The phosphonate-based ligands have a strong affinity for uranium, and they have been applied in uranium separation by adsorption [81–84], the modified water-soluble polymers and copolymers based on phosphoric acid ligands are thus promising for the uranium chelation and the application in the complexation assisted ultra/nanofiltration.

Phosphonic acids (R-PO_3H_2) are diprotic, with $pK_{a1} \approx 2$–3 and $pK_{a2} \approx 6$–7 [85]. Above pH 2, the first proton dissociates, imparting a negative charge that enhances electrostatic attraction to metal cations and increases polymer hydrophilicity, thereby accelerating sorption. Between pH 2 and pH 7 (i.e., between pK_{a1} and pK_{a2}), phosphonic acid moieties act both as chelating ligands forming coordination complexes and as polyelectrolytes providing electrostatic interactions, resulting in dual sorption mechanisms. Above pH 7, both protons are dissociated and sorption is dominated by electrostatic binding of U(VI) species. Below pH 2, the phosphonic groups remain protonated and sorption relies solely on coordination bonds, although overall capacity decreases due to proton competition [85]. Previous studies confirm the high affinity of phosphonic functionalities for uranium. Prabhakaran et al. reported a maximum U(VI) uptake of 1.38 mmol g^{-1} on a phosphonic-derivatized resin [86], while Vasudevan et al. demonstrated effective seawater U (VI) recovery using cross-linked methacrylate membranes bearing both sulfonic and phosphoric groups [87]. These polymers were selected for their performances in uranium decontamination with the same principles published in the works of A. Graillot et al [88,89].

The synthetized polymers (**I, II**) can form gels. The gelation is caused by the loss of water solubility of their heat sensitive (initially hydrophilic) part, which occurs above a certain threshold temperature, called the lower critical solubility temperature (Lower Critical Solution Temperature or LCST). Above this temperature, the polymer-solvent interactions (hydrogen bonds formed between the polar parts of the polymer and the water) are unfavourable and the macromolecules aggregate to cause phase separation. The value of the LCST depends on the nature of the polymer. It is typically around 32 °C for poly(NiPAAM), the heat sensitive part of the copolymers of **I** and **II**.

Poly(ethylene glycol) functionalized with bis(phosphonic acid) moieties (**III**) is anticipated to exhibit strong U(VI) complexation due to its high density of phosphonic acid groups, which are known to bind uranyl ions with high affinity [72,90–92]. Similarly, catechol-based ligands (**IV**) form exceptionally stable complexes with U(VI), with reported formation constants on the order of 10^{14} [93], making catechol-terminated polymers promising candidates for selective uranium capture.

3.2. Rejection kinetics

The time required to achieve optimal uranium selectivity varies among polymers, reflecting differences in polymer–U complexation kinetics. During each filtration run, retentate and permeate samples were collected at 30 min intervals up to 3.5 h, the rejection of uranium and competing salts were determined. Conditions for each polymer, including uranium and polymer concentration, membrane MWCO, are detailed in Table 1. Fig. 3(a-f) and Table S.8 show the rejection profiles of uranium and metal ions for all six polymers, enabling direct comparison of their selectivity dynamics.

Complexation-assisted filtration trials were performed using Mediterranean seawater spiked with 20 mg L^{-1} U (VI) to assess each polymer's uranium-binding efficiency and its selectivity over competing cations. Table 2 summarizes the kinetic results, reporting for each polymer the time at which the U/Na separation factor peaked, together with the corresponding rejection percentages for U and other salts. Separation factors, $SF_{(U/metal)}$, were calculated as the ratio of distribution coefficients, K_d(U) and K_d(metal).

$$SF_{(U/metal)} = \frac{K_d(U)}{K_d(metal)} \tag{2}$$

K_d is calculated with the formula:

$$K_d = \frac{m_i - m_f}{m_f} \times \frac{V_p}{m_p} \tag{3}$$

with m_i and m_f respectively the initial and final mass of uranium in permeate, V_p the volume of permeate, m_p the mass of polymer.

With no polymer present, membranes reject essentially 0 % of all metal ions in seawater (Fig. 3) [44]. Introducing a chelating polymer dramatically boosts uranium rejection by steric exclusion—regardless of how many binding sites or what net charge the U–polymer complex carries—because the polymer's molecular weight always exceeds the membrane's MWCO. Moreover, at seawater salinity (35 g L^{-1}), electrostatic effects are fully screened, so rejection directly reflects the fraction of metal ions bound to polymer. By "enlarging" uranium into high-molecular-weight complexes, hydrophilic polymers achieve selective separation. 1 kDa membrane paired with a 2 kDa polymer or a 5 kDa membrane with a 40 kDa polymer both exploit this steric mechanism, although the 5 kDa system offers higher flux and lower fouling. Fig. 3(a) shows that with polymer **I-A** (1 g L^{-1}) and U at 20 mg L^{-1}, uranium rejection initially spikes to 95 % after 30 min, then falls to 54 % at 60 min and stabilizes around 40 % after 2 h, other salts follow a similar decline to 20–40 %. This limited performance stems from the fact that **I-A** hass relatively few alendronate complexing sites. As shown in Fig. S.7, under the defined "solution 1" conditions (20 mg L^{-1} U, 35 g L^{-1} NaCl, 0.84 g L^{-1} $NaHCO_3$), polymer **I-B** at 1 g L^{-1} achieved ~96 % U rejection and ~ 6 % Na rejection. This corresponds to a separation factor SF(U/Na) of 432. Despite the more complex ionic composition of natural seawater, **I-B** delivered even higher uranium-to-salt selectivity, when applied to it, underscoring its robustness in realistic matrices. Fig. 3(b)

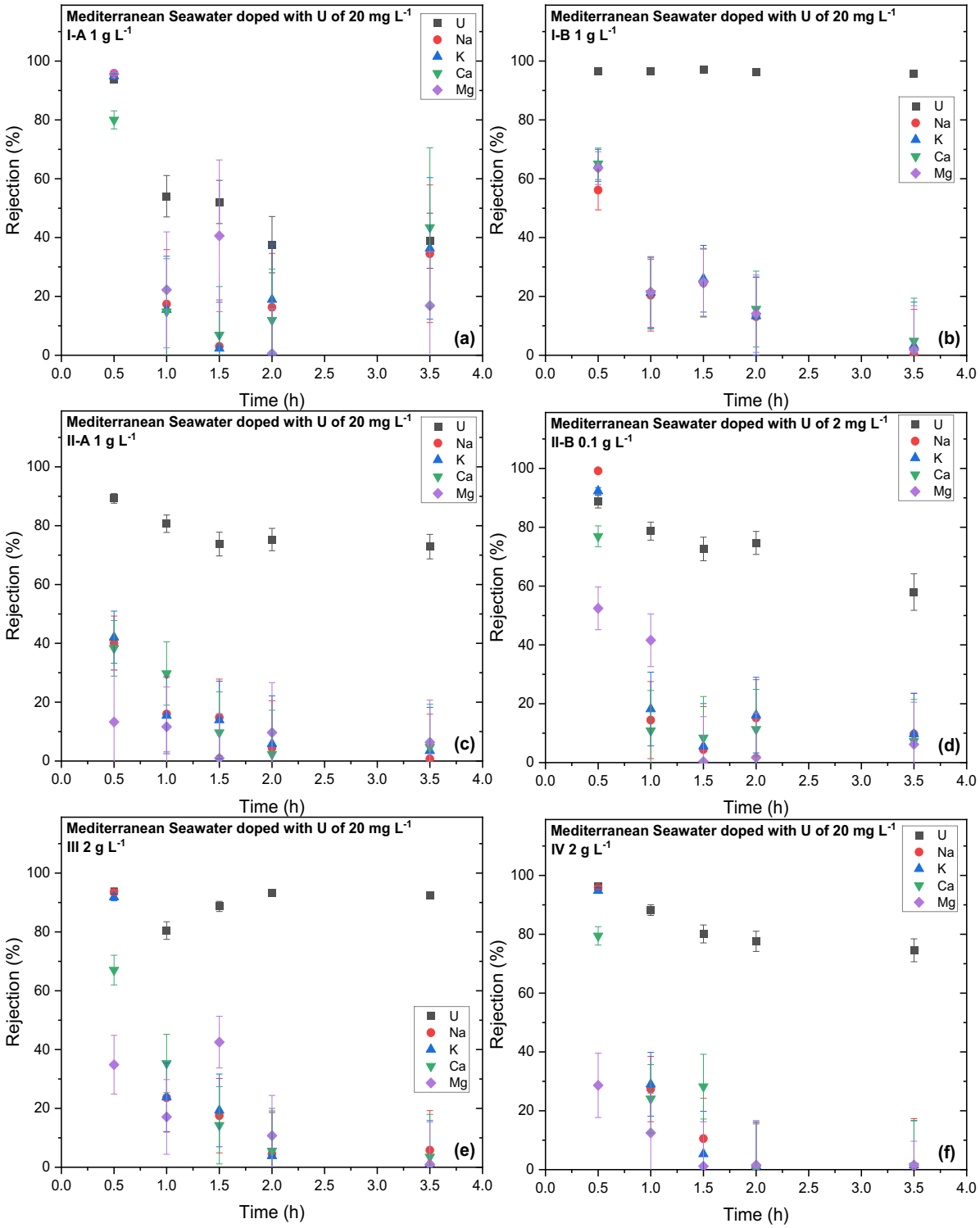

Fig. 3. Filtration assisted by complexation of (a) Mediterranean seawater spiked with 20 mg L^{-1} of uranium with **I-A** of 1 g L^{-1}; (b) Mediterranean seawater spiked with 20 mg L^{-1} of uranium with **I-B** of 1 g L^{-1}; (c) Mediterranean seawater spiked with 20 mg L^{-1} of uranium with **II-A** of 1 g L^{-1}; (d) Mediterranean seawater spiked with 2 mg L^{-1} of uranium with **II-B** of 0.1 g L^{-1}; (e) Mediterranean seawater spiked with 20 mg.L^{-1} of uranium with **III** of 2 g L^{-1}; (f) Mediterranean seawater spiked with 20 mg L^{-1} of uranium with **IV** of 2 g L^{-1}.

demonstrates that polymer **I-B** (1 g L^{-1}) maintains ~96 % uranium rejection for3.5 h, while the rejection of Na^+, K^+, Ca^{2+}, and Mg^{2+} decrease from ~60 % to <5 %. The higher density of phosphonate sites in **I-B** thus delivers excellent selectivity, overcoming the hindrance of high ionic strength through steric exclusion alone [44]. In complex seawater, the uranium–phosphonate chelation system benefits from several synergistic effects that amplify the U/Na selectivity compared to a simple NaCl–HCO_3^- solution. First, the multitude of weakly coordinating ions (K^+, Mg^{2+}, Ca^{2+}, and trace metals) "share" low-affinity binding sites, so Na^+ occupies fewer sites by mass action, leaving more high-affinity sites available for UO_2^{2+}. Second, divalent cations and additional monovalent ions distort the local ion atmosphere at the

Table 2
Rejection of U with each polymer at the steady state of filtration in the kinetics study with seawater spiked with U at 20 mg L^{-1}.

Polymer	Without polymer [44]	I-A	I-B[a]	I-B	II-A	II-B	III	IV
Molar mass (g mol^{-1})	–	31,400	36,300	36,300	42,200	47,150	2200–2285	2000–2100
[Polymer] (g L^{-1})	–	1	1	1	1	0.1	2	2
t_{max} (h)	–	1.5	1	3.5	3.5	1.5	2	2
RE (U) (%)	0	52.1	96.3	95.7	72.9	72.6	93.2	77.6
RE (Na) (%)	0	3.0	5.7	0.3	0.7	4.4	4.5	0.7
RE (K) (%)	0	2.3	–	3.2	3.5	5.6	3.9	1.2
RE (Mg) (%)	0	40.6	–	1.8	6.4	0.4	10.7	1.6
RE (Ca) (%)	0	6.9	–	4.8	4.7	8.4	5.6	0.2
SF_{max} (U/Na)	1	35	432	6856	363	61	289	488
SF_{max} (U/K)	1	45	–	665	75	47	341	280
SF_{max} (U/Mg)	1	2	–	1223	39	790	114	215
SF_{max} (U/Ca)	1	15	–	438	54	31	234	1603

t_{max} denotes the filtration time at which the U/Na separation factor reaches its maximum.
RE represents the rejection efficiency of the specified metal ion at t_{max}.
SF_{max} is the highest separation factor achieved during the filtration experiment.
[a] Experiment was conducted with the solution 1; all the other experiments were conducted with seawater doped with U at 20 mg L^{-1}.

polymer interface, effectively reducing the concentration of Na^+ near the binding sites and further limiting its weak association. Third, high Mg^{2+}/Ca^{2+} concentrations induce polymer chain collapse or aggregation via charge screening and cross-linking. This results in a tighter network in which only strongly binding, multidentate UO_2^{2+} species can penetrate and coordinate. Consequently, the sodium ability to "soak up" polymer sites is significantly reduced, allowing uranium to predominantly occupy the available phosphonate groups and driving the SF(U/Na) in real seawater to values that are an order of magnitude higher than in binary NaCl–HCO_3^- media.

The kinetics of uranium and salt rejection by polymer **II-A** (1 g L^{-1}) at 20 mg L^{-1} U in seawater are shown in Fig. 3(c). Both uranium and competing salts reached peak rejections of 90 % and 40 % respectively within the first 30 min, then declined to steady values by 2 h—approximately 75 % for U and below 10 % for salts. Optimal selectivity (U rejection ≈75 %; salts <10 %) occurred at 2 h and persisted through 3.5 h. Fig. 3(d) presents the rejection profile for polymer **II-B**, tested at 0.1 g L^{-1} with 2 mg L^{-1} U. Uranium rejection fell from 90 % at 30 min to 73 % at 1.5 h and stabilized around 75 % until 2 h, before dropping to 58 % by 3.5 h. This lower performance relative to **I-B** likely reflects the reduced polymer and uranium concentrations. In experiments for sorption capacity determination, however, 0.5 g of **II-B** with 20 mg L^{-1} U in 1 L of seawater achieved 96 % rejection, comparable to **I-B**, confirming the efficacy of the alendronic acid functionality.

At a polymer loading of 2 g L^{-1} and U(VI) concentration of 20 mg L^{-1} in seawater, polymer **III** achieved 94 % uranium rejection within the first 30 min. Optimal selectivity (93 % U versus <11 % rejection of other salts) was reached after 2 h of filtration (Fig. 3(e)). Under identical conditions, polymer **IV** delivered 78 % U rejection and <2 % rejection of competing ions at 2 h; however, Mg^{2+} rejection rose to 47 % by 3.5 h (Fig. 3(f)).

Among all hydrophilic polymers tested, **I-B** showed the highest uranium affinity and selectivity in high-salinity seawater, achieving 96 % U rejection while limiting monovalent and divalent salt rejection to below 5 % (1 g L^{-1} polymer, 20 mg L^{-1} U). Its separation factors for U/Na^+, U/K^+, U/Mg^{2+}, and U/Ca^{2+} were 6856, 665, 1223, and 438, respectively. In contrast, **I-A** exhibited poor selectivity (SF(U/Na^+) = 35; SF(U/Mg^{2+}) = 2).

At a polymer concentration of 2 g L^{-1} and U at 20 mg L^{-1} in seawater, polymer **III** reached 94 % uranium rejection within the first 30 min, with optimal selectivity, 93 % U versus <11 % other salts, observed after 2 h of filtration (Fig. 3(e)). Under the same conditions, polymer **IV** achieved 78 % U rejection and <2 % rejection of competing salts at 2 h. However, Mg^{2+} rejection increased to 47 % by 3.5 h (Fig. 3(f)).

Upon introduction of polymers into the uranium-spiked seawater, membrane rejection exhibits a characteristic two-stage profile (Fig. 3). In the initial 30 min, all polymers form large, polymer–ion assemblies, either strong U(VI) chelates or weaker complexes with Na^+, K^+, Ca^{2+}, and Mg^{2+} which exceed the membrane MWCO, resulting in high rejection of uranium (80–95 %) and substantial co-rejection of competing salts (20–60 %) because they're swept up in the polymer matrix or in the nascent fouling layer. As filtration proceeds beyond 1 h, weaker polymer–salt interactions desorb or permeate, while the robust U–polymer chelates remain oversize and continue to be sterically excluded. Consequently, monovalent and divalent salt rejection steadily falls below 10 %, whereas uranium rejection stabilizes at a high level (75–96 %), with the exact value dictated by the chelator's binding density and affinity. For example, **I-B** and **II-A** maintain >90 % U rejection and < 5 % salt rejection after 3.5 h, reflecting their strong phosphonate and alendronic acid functionalities, whereas lower-density polymers (e.g., **I-A**, **IV**) show a gradual decline in U retention as binding sites saturate or polymers shear from the membrane surface. This two-stage behavior underscores the necessity of at least 1.5–2 h of operation to achieve good uranium selectivity, highlighting the critical role of high-affinity, high-molecular-weight chelators in overcoming seawater's ionic complexity. In an open-cycle UF/NF industrial setup, where feed continuously enters and permeate and retentate streams are drawn off without being recycle back to the feed tank, U(VI) bound to the polymer is completely rejected by the membrane and accumulates in the retentate. Conversely, uncomplexed salts freely permeate and are collected in the permeate stream. Over time, this separation mechanism progressively enriches U in the retentate, achieving significantly elevated U concentrations while maintaining low salt content.

3.3. Sorption capacity

It is particularly important to evaluate the sorption capacity of the polymers in order to scale up the filtration process to an industrial scale. However, on a laboratory scale, it is challenging to continuously pump seawater through a small filtration system with a feed tank of 1 L. Despite the limitation, sorption capacity can be estimated by filtering seawater with a fixed quantity of polymer while continuously doping U into the feed seawater to simulate the introduction of U from a new seawater source. This filtration procedure has various advantages. Firstly, the continuous filtration mimics real industrial conditions where sea waves come to the filtration membrane. Secondly, maintaining a fixed polymer concentration throughout thefiltration process is beneficial to economize polymer.

Fig. 4 presents representative sorption-capacity experiments, showing uranium rejection and corresponding sorption capacity as a function of initial U concentration. Complete datasets for all sorption-capacity trials are available in the Supporting Information (Tables S.9, S.10, S.11 and Figs. S.8 to S.12). Under seawater conditions, yellow-

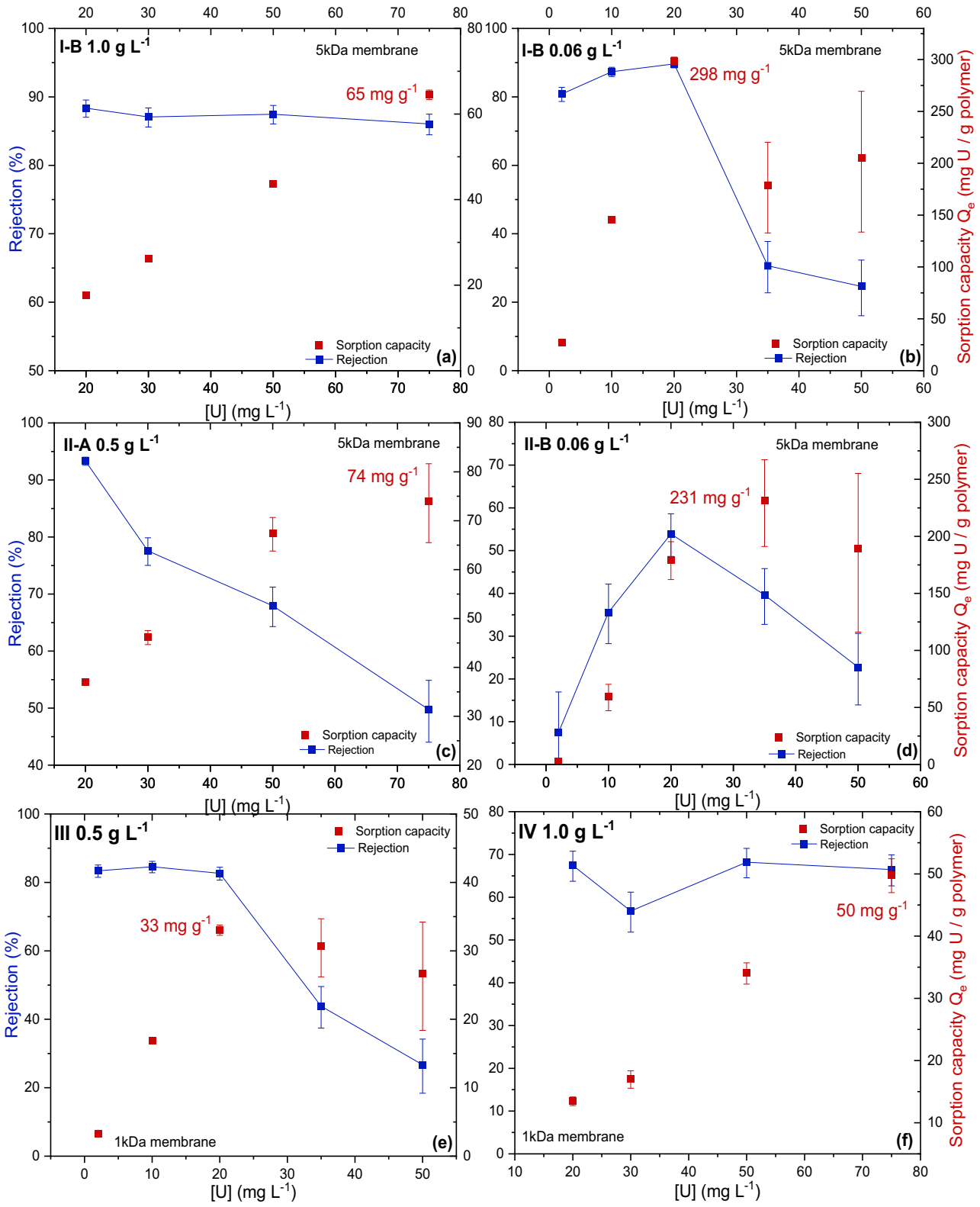

Fig. 4. (a) Rejection of U and sorption capacity Qe(U) by UF/NF assisted by polymer **I-B** (C = 1 g L^{-1}) as a function of uranium concentration (20 to 75 mg L^{-1}); (b) Rejection of U and sorption capacity Qe(U) by UF/NF assisted by polymer **I-B** (C = 0.06 g L^{-1}) as a function of uranium concentration (2 to 50 mg L^{-1}); (c) Rejection of U and sorption capacity Qe(U) by UF/NF assisted by polymer **II-A** (C = 0.5 g L^{-1}) as a function of uranium concentration (20 to 75 mg L^{-1}); (d) Rejection of U b and sorption capacity Qe(U) y UF/NF assisted by polymer **II-B** (C = 0.06 g L^{-1}) as a function of uranium concentration (2 to 50 mg L^{-1}); (e) Rejection of U and sorption capacity Qe(U) by UF/NF assisted by polymer **III** (C = 0.5 g L^{-1}) as a function of uranium concentration (2 to 50 mg L^{-1}); (f) Rejection of U and sorption capacity Qe(U) by UF/NF assisted by polymer **IV** (C = 1.0 g L^{-1}) as a function of uranium concentration (20 to 75 mg L^{-1}).

green precipitation showed when U concentration surpassed 75 mg L^{-1}. However, in the experiment with **II-B**, no precipitation occured even when C_f reached to 175 mg L^{-1}. When precipitates were present, sorption capacity was no longer measurable. These precipitates could consist of various minerals such as UO_2CO_3, (Na, Ca, Mg)-UO_2-CO_3·xH_2O, including Liebigite ($Ca_2(UO_2)(CO_3)_3$·10H_2O), Swartzite ($CaMg(UO_2)(CO_3)_3$·12H_2O), Bayleyite ($Mg_2(UO_2)(CO_3)_3$·18H_2O), or Andersonite ($Na_2Ca(UO_2)(CO_3)_3$·6H_2O) [94].

The sorption capacity is calculated with the following formula:

$$Q_e = \frac{m_r}{m_p} \tag{4}$$

where m_r is the mass of uranium rejected (uranium complexed with polymer) in the filtration experiment, and m_p is the mass of polymer added to the seawater.

Figs. S.8 to S.12 gather the uranium uptake (Qe) versus residual concentration (Ce) plots for every polymer–dose combination and superimposes the Langmuir (L) and Freundlich (F) regressions. The fit statistics are compiled in Tables S. 9, S. 10 and S. 11, only one set of values is quoted when R_L^2 and R_F^2 differ by <0.03, otherwise the better model is highlighted.

Both **I-B** and **II-B** complex U(VI) through the same alendronate (ALNAm) groups, which allows complexation through coordination (P═O functions) or ion exchange (hydroxyl functions carried by the P-O-H through a proton exchange against a metal cation) [95], but their distinct architectures yield markedly different sorption behaviors. In **II-B**, the alendronate (ALNAm) units are sequestered within a hydrated, brush-like shell that remains fully accessible under crossflow, enabling sustained, high-capacity uranium uptake. The high local ligand density and full hydration minimise steric hindrance, giving the highest validated capacity (496 mg g^{-1} at 0.50 g L^{-1}) with matching Langmuir/Freundlich quality (R_L^2 = 0.94, R_F^2 = 0.96), indicating a quasi-homogeneous population of bis-phosphonate sites in the NAM/ALNAm hydrated shell, achieving the best experimentally confirmed capacity in this study. At 0.08 g L^{-1} the shell is still unsaturated, Qe climbs from 113 to 382 mg g^{-1} while Ce increases only four-fold, forcing the Langmuir asymptote out to 2.7 g g^{-1}. This value therefore represents the theoretical potential rather than a practical design figure. A dose of 0.06 g L^{-1} gives a lower plateau (289 mg g^{-1}) and poorer fits (R_L^2 = 0.76), because the last two points were still approaching equilibrium at the 4 h mark. In **I-B**, the same ALNAm units are randomly distributed along the NAM backbone. Random NAM/ALNAm scatters the ligand along the chain, the spatial density is lower and after a few phosphonate groups chelate UO_2^{2+} the coil collapses locally, the macromolecule collapses around the metal ion, sterically shielding the remaining sites. Consequently, **I-B** saturates at ≈310 mg g^{-1} even with 1 g L^{-1} polymer, though the affinity remains excellent (b = 2.5 × 10^{-2} L mg^{-1}), confirming that statistical dispersion of ALNAm lowers the site density yet leaves the intrinsically strong U–phosphonate bond intact. Reducing the dose to 0.06 g L^{-1} inflates the apparent affinity to 1.8 L mg^{-1} but drops R_L^2 to 0.46, clear evidence that 4 h are insufficient for full equilibration at such a low polymer/U ratio. Compared to **II-B**, the superior experimental capacity of **I-B** arises from its higher bis-phosphonate site density (0.364 vs. 0.280 g site g^{-1} polymer) and the additional amide functionalities in **II-B**, which further stabilize U(VI) via solvation and metal–oxygen coordination. The amide function in **II-B** also contributes to U complexation through solvation [96] and coordination metal-O bond [97], similar to alendronic acid. However, the primary complexing properties of these polymers are due to alendronate [98]. The performance divergence between **II-B** and **I-B** underscores the importance of micro-segregation of binding sites. **II-A**, identical to **II-B** except for a shorter NIPAAm block, reaches only 73 mg g^{-1}. The high Freundlich exponent (n = 4.4) indicates a narrow distribution of high-energy sites that saturate early. Increasing dose, not extending chain length, is therefore required to create new available sites. Polymer **III** presents its chelating ligands exclusively at the chain termini. Its plateau was 32, 65, and 139 mg g^{-1} when the dose was respectively 0.5, 1 and 0.1 g L^{-1}. The affinity b follows the opposite trend, falling from 0.97 to 0.025 L mg^{-1} as the few high-energy end groups become titrated. **IV** remains strictly linear over 6–25 mg L^{-1} (n = 0.88), the catechol population is evidently too small to reveal a plateau in this concentration window.

Overall, sorption isotherms exhibiting true plateaus—namely **II-A**, **II-B** at 0.50 g L^{-1}, and **III** at 1 g L^{-1}—are best described by the Langmuir model, indicating a largely uniform population of high-affinity binding sites. In contrast, Freundlich behavior dominates at lower polymer doses for **II-B** and **III**, where the highest-energy sites are occupied first and progressively weaker interactions emerge as C_e increases. The equivalent R^2 values observed for **II-B** at 0.08 g L^{-1} and **I-B** at 1 g L^{-1} suggest that, in these cases, a single sorption mechanism prevails but is superimposed upon a modest degree of site heterogeneity.

3.4. Desorption

A pH-driven desorption step with UF/NF was implemented to remove uranium from the U-polymer complexes by adjusting the pH of the seawater retentate. In these trials, seawater retentate containing U–polymer complexes was acidified with 0.1 M HNO_3 (Table 3), which protonated the phosphonate and amide binding sites and shifted the complexation equilibrium, releasing UO_2^{2+} into solution, as evidenced by the reduced rejections. The acidic medium allows on one hand the reprotonation of the complexing functions of the hydrophilic polymers and on the other hand shifts the thermodynamic equilibrium of complexation. During the subsequent UF/NF stage, the oversized polymer chains were sterically retained, while liberated uranium and the background salts permeated the membrane (Fig. 5(a)). High seawater ionic strength surpassed electrical effect, ensuring that permeation was governed solely by molecular size.

By adding concentrated HNO_3 and adjusting the concentration to 0.1 mol L^{-1} for the retentate with **II-B**, the rejection of U decreased to 12.6 %, compared to its initial rejection of 97 % in the filtration-complexation step. For **IV**, U rejection dropped from 75 % to 5.9 % during desorption. For **II-A** and **III**, approximately 15 % of U remained complexed with the polymer. The U rejection of U with **I-B** during desorption was notably high at 67 %, compared to 86.1 % in the filtration-complexation step, indicating that only 19.5 % of the complexed U was released from the complex under this acidic environment of HNO_3 at 0.1 mol L^{-1}. This stability suggests that increasing the acidity or using different acidic solutions might be necessary to dissociate more U from **I-B**.

The acid dissociation constants (pKa) of each polymer are summarized in Table S.5 [99–101]. The main complexing functional group for **I-B**, **II-B**, and **II-A** is alendronic acid, while phosphonic acid and catechol are the functional groups for **III** and **IV**, respectively. Compared to other polymers, the PEG-catechol system (**IV**) facilitates easier desorption of uranium, as the hydroxyl functional groups complexed with uranium are protonated at higher pH values, making decomplexation more efficient. However, these pKa values are only indicative of each polymer's

Table 3
Rejection of uranium in desorption filtration of seawater spiked with HNO_3 at 0.1 mol L^{-1}.

Hydrophilic polymer	[polymer] (g L^{-1})	[U] (mg L^{-1})	R_ini (%)	R_back (%)
I-B	0.06	50	86.1	66.6
II-A	0.5	75	49.7	15.9
II-B	0.06	50	97.0	12.6
III	1	75	70.6	14.7
IV	2	20	75.0	5.9

R_ini: the rejection of U in the filtration experiment of kinetics or sorption capacity study.
R_back: the rejection of U in the desorption filtration experiment.

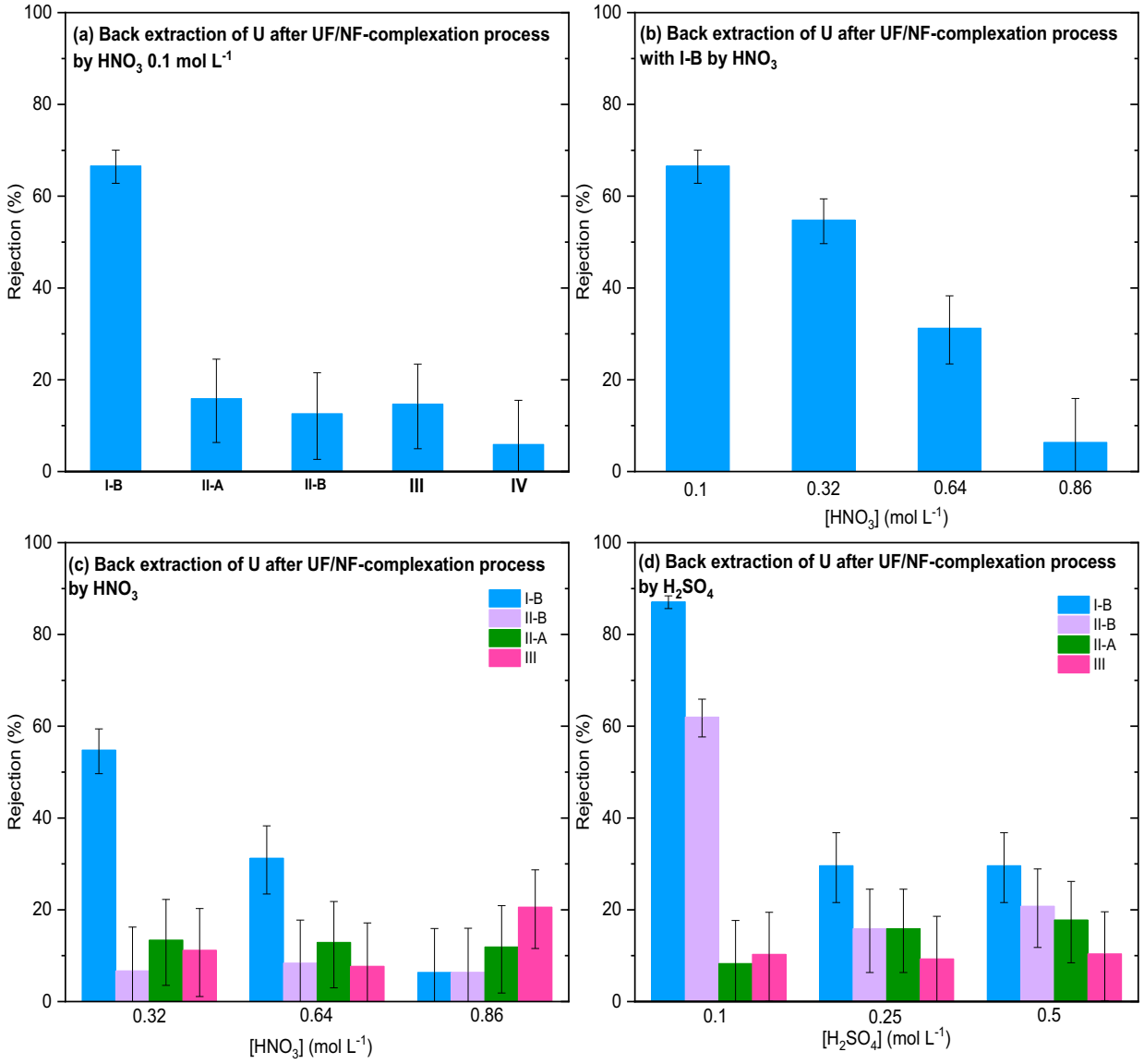

Fig. 5. (a) Rejection of uranium in desorption filtration with nitric acid medium 0.1 mol L^{-1} with **I-B**, **II-A**, **II-B**, **III** and **IV**; (b) rejection of uranium in desorption with **I-B** as a function of nitric acid concentration; (c) rejection of uranium in desorption filtration with **I-B**, **II-B**, **II-A** and **III** as a function of nitric acid concentration; (d) rejection of uranium as a function of H_2SO_4 concentration in desorption filtration with **I-B**, **II-B**, **II-A**, and **III**.

desorption ability and do not account for modifications introduced by grafting these functional groups onto a polymer.

To improve uranium release from **I-B**, desorption was performed across a range of nitric acid concentrations. Fig. 5(b) shows the variation of U rejection with [HNO_3] during desorption of a 50 mg L^{-1} U solution at 0.06 g L^{-1} **I-B** loading. As acidity increased, U rejection declined markedly, from 66 % at 0.10 M HNO_3 to 6 % at 0.86 mol L^{-1}—reflecting progressive decomplexation of UO_2^{2+} and effective liberation of uranium from the polymer matrix. The observed dependence of desorption efficiency on acid strength further underscores that efficient decomplexation requires sufficient reprotonation of **I-B**'s alendronic acid sites. The same experiment was carried out on **II-A**, **II-B** and **III** to assess the impact of nitric acid concentration on U desorption. The results, depicted in Fig. 5(c) and detailed in Table S.7, indicate that **II-A** and **II-B** exhibited no significant change in U rejection even at the highest acid concentrations tested, indicating complete destabilization of their U–polymer complexes at 0.1 M HNO_3. Polymer **III** showed a non-monotonic trend, with minimum U rejection at 0.64 mol L^{-1} and a rebound at 0.86 mol L^{-1}, likely an artifact of measurement variability. Overall, these results confirm that the **I-B**–uranium complex is the most acid-stable of those studied, requiring elevated [HNO_3] (>0.8 mol L^{-1}) for efficient decomplexation, whereas **II-A**, **II-B**, and **III** achieve near-complete U desorption at 0.1 M HNO_3.

Sulfuric acid was also assessed as an alternative desorption agent, whereas hydrochloric acid was avoided due to corrosion concerns with our stainless-steel filtration hardware [102]. Desorption trials were performed on seawater retentates using the polymer loadings listed in Table S.6 and across H_2SO_4 concentrations of 0.10 to 0.50 mol L^{-1}. As shown in Fig. 5(d) and Table S.7, U rejection by **I-B** declined from its complexation-step value as [H_2SO_4] increased to 0.25 mol L^{-1}, then plateaued between 0.25 and 0.50 mol L^{-1}. **II-B** exhibited a similar initial decrease in rejection up to 0.25 mol L^{-1}, followed by a slight rebound at 0.50 mol L^{-1}. Both acids proved highly effective for uranium release from polymer **III**, yielding consistently low rejection (~10 %) regardless of [H_2SO_4]. Overall, sulfuric-acid desorption (0.10–0.50 M) produced higher U rejections—and hence lower apparent desorption efficiencies—than nitric-acid elution over the comparable molarity range (0.32–0.86 M). From these data, we identify 0.1 M H_2SO_4 as the most efficient desorption condition for **II-A**, while **II-B** and **I-B** require stronger eluents: 0.32 M HNO_3 and 0.86 M HNO_3, respectively, to

achieve maximal uranium recovery.

Sulfuric acid was expected to facilitate U(VI) release more effectively than nitric acid, given the strong formation constants of uranyl–sulfate species (see Supporting Information). However, desorption trials revealed consistently higher uranium rejection, and thus lower apparent release with H_2SO_4 than with HNO_3 at comparable molarities. This unexpected result could be attributed to the salting out effect caused by the high concentration of SO_4^{2-}. As a strong kosmotrope in the Hofmeister series, sulfate promotes water structuring and stabilizes intramolecular interactions in macromolecules, inducing collapse of the PNIPAm backbone in **II-B** [103–106]. This folding restricts access to alendronic acid sites, impeding their reprotonation and the subsequent liberation of UO_2^{2+}. In contrast, chaotropic anions would tend to swell the polymer network and enhance site accessibility. Therefore, kosmotropic conditions, while beneficial for certain protein-stabilization applications, undermine the efficiency of sulfate-based desorption by reinforcing polymer collapse and inhibiting the decomplexation necessary for uranium release.

The distribution of uranium (U) species in seawater spiked with 20 mg L^{-1} U with 0.1 mol L^{-1} of HNO_3 and the same solution with 0.1 M H_2SO_4, simulated with PHREEQC software, is depicted in Fig. S.23(a) and (b), respectively. The speciation plots, although limited to inorganic equilibria, nevertheless offer valuable mechanistic insight. In 0.1 M HNO_3 (Fig. S.23(a)), approximately 59 % of dissolved uranium is predicted to exist as free UO_2^{2+}, with only ~12 % as UO_2Cl^+ and ~27 % as UO_2SO_4. Because nitrate forms negligible uranyl complexes, these data imply that HNO_3 desorption proceeds primarily via protonation of the polymer's phosphonate sites, releasing true UO_2^{2+} (or weakly coordinated UO_2Cl^+) that then permeates the membrane. By contrast, in 0.1 M H_2SO_4 (Fig. S.23(b)), <15 % of uranium remains as UO_2^{2+}, while the majority (~82 %) partitions into UO_2SO_4 and $UO_2(SO_4)_2^{2-}$ complexes. These small sulfate species readily traverse the membrane and indicate that competitive ligand substitution by SO_4^{2-} contributes substantially to uranium release under acidic sulfate conditions. Moreover, the high sulfate concentration likely induces PNIPAm chain collapse via kosmotropic salting-out, further impeding proton-only decomplexation. Although these simulations do not include polymer–uranyl binding, they robustly support the conclusion that nitric-acid desorption is dominated by site reprotonation, whereas sulfuric-acid desorption combines protonation with significant uranyl–sulfate ligand exchange. Future work coupling inorganic speciation models with simple polymer binding terms, as well as post-desorption quantification of polymer-bound uranium (e.g., by size-exclusion chromatography), would enable full deconvolution of these pathways and guide optimized eluent design.

3.5. Blank experiments

Blank experiments were carried out to demonstrate that the high rejection of U under acidic conditions arises from polymer decomplexation rather than electrostatic exclusion with polymer in seawater. Filtration of seawater spiked with 20 mg L^{-1} UO_2^{2+} was performed for 4 h on a 1 kDa membrane in the presence of either 0.1 M HNO_3 or 0.1 M H_2SO_4, but without polymer. Both acids yielded similar rejection: 9.2 % for HNO_3 and 10.5 % for H_2SO_4. These low, nearly identical values demonstrate that membrane charge effects are fully screened at high ionic strength and that residual uranium retention under acidic pH is negligible in the absence of polymer.

As shown in the species distribution diagram of uranium (U) species in seawater spiked with 20 mg L^{-1} U with 0.1 M HNO_3 and the same solution with 0.1 M H_2SO_4 (Fig. S.23(a) and (b)), In the nitric-acid system, ~60 % of dissolved uranium exists as UO_2^{2+}, whereas in the sulfate system >80 % is present as UO_2SO_4 and $UO_2(SO_4)_2^{2-}$. If electrostatic exclusion played a role, one would expect high U rejection in the UO_2^{2+}-dominated nitric-acid feed and negligible rejection in the sulfate feed. Instead, blank filtrations yielded similarly low U rejections, confirming that charge effects are fully screened at seawater ionic strength. This indicates that any electrical effect is effectively shielded, consistent with findings on seawater's high ionic strength reported previously [44]. In seawater adjusted to 0.1 M HNO_3 or H_2SO_4, the addition of polymer elevates uranium rejection (>60 % for **I-B**), compared to only ~10 % rejection in polymer-free controls under identical conditions. This stark contrast confirms that electrostatic effects are negligible at high ionic strength, and that uranium retention arises from steric exclusion of the high-molecular-weight U–**I-B** complex.

In summary, uranium desorption from the U–polymer complex is achieved by acidifying the retentate with a concentrated acid. While both HNO_3 and H_2SO_4 can effectively reprotonate binding sites and release U(VI), the choice of acid requires careful consideration of operational constraints. In particular, HNO_3 is generally favored in 316 L stainless-steel systems due to its substantially lower long-term corrosion risk relative to H_2SO_4 [107–109]. Importantly, the strong acid eluent does not compromise membrane integrity or polymer functionality. However, preliminary polymer-regeneration trials (Supporting Information) have highlighted corrosion issues in our 316 L stainless-steel filtration rig, likely exacerbated by repeated exposure to seawater, ageing materials, and the use of highly acidic desorption solutions.

4. Conclusions and perspectives

This study explores the feasibility of using inorganic membranes for separating or concentrating uranium from seawater through ultra/nanofiltration-complexation processes facilitated by hydrophilic polymers featuring different complexing functional groups (alendronic acid, bis(phosphonic acid), catechol). It encompasses investigations into rejection kinetics, sorption capacities, and the subsequent desorption of uranium. Key findings include the identification of steric repulsion as the primary mechanism driving uranium rejection in complexation-assisted filtration. At seawater ionic strength (35 g L^{-1}), electrostatic exclusion is negligible. Instead, high-molecular-weight U–polymer assemblies are sterically retained (up to 96 % U rejection), while Na^+, K^+, Ca^{2+} and Mg^{2+} pass through (<5 % rejection). The selection of hydrophilic polymers with high uranium sorption capacities proves crucial for effective separation. Among the six polymers tested, **I-B** and **II-B**, exhibit exceptional performance, achieving maximum sorption capacities exceeding 200 mg U/g polymer and remarkably high uranium-to-salt separation factors ($SF_{(U/Na)}$ > 6000 for **I-B**). Polymers **III** and **IV** also demonstrate high uranium-to-salt separation factors. Concentrated HNO_3 (0.1–0.86 M) or H_2SO_4 (0.1–0.5 M) reprotonates the chelating sites and release UO_2^{2+} into the permeate without damaging the integrity of the inorganic membrane. HNO_3 is preferred in 316 L stainless steel systems due to lower corrosion risk. While our laboratory results demonstrate the technical feasibility and high selectivity of polymer-assisted UF/NF for uranium recovery from seawater, comprehensive techno-economic and environmental assessments are still needed. Future work will include pilot-scale trials to gather real-world data on polymer and membrane consumption, energy and acid usage, and process yields. In summary, with its high efficiency and easy feasibility, the complexation-assisted filtration process is promising for uranium preconcentration from seawater due to its high efficiency and ease of implementation, thereby streamlining subsequent concentration steps.

Despite the promising results obtained under controlled laboratory conditions, several critical challenges must be addressed before the technology can be considered viable for industrial-scale implementation.

One of the foremost challenges is demonstrating trace-level performance in natural seawater. While laboratory experiments often rely on artificially spiked uranium concentrations at the milligram-per-liter level, real-world applications must contend with the much lower natural uranium concentration of approximately 3.3 μg L^{-1}. Therefore, it is essential to conduct adsorption trials across a realistic concentration

range (1–100 μg L^{-1}), using inductively coupled plasma mass spectrometry (ICP-MS) for precise quantification. These trials will provide more accurate adsorption isotherms, including maximum adsorption capacity (Q_{max}) and binding affinity, as well as separation factors (SF) in the presence of competing ions such as calcium, magnesium, iron, molybdenum, vanadium, and various organic fragments. This approach will help identify any overestimations of selectivity that may have occurred under simplified laboratory conditions.

Another key consideration is the long-term operational stability of the system. Continuous ultrafiltration (UF) and nanofiltration (NF) experiments extending beyond 24 h are necessary to evaluate the durability of the polymer materials, the extent of flux decline, and the susceptibility of membranes to fouling under realistic feed conditions. Monitoring the retention of adsorption capacity and any drift in rejection performance over multiple days will provide critical insights into the frequency of cleaning cycles, the need for polymer re-dosing, and the design of filtration modules for sustained operation.

The purity of the recovered uranium is also a major concern, particularly with respect to downstream processing. During acid elution, it is important to quantify the co-desorption of vanadium, iron, and organic fragments using ICP-MS and total organic carbon (TOC) analysis. To achieve nuclear-grade uranium purity, it may be necessary to integrate secondary purification steps such as selective precipitation, ion exchange, or a tightly configured NF/reverse osmosis (RO) cascade following the initial desorption process.

Cyclability and material durability must also be rigorously tested. Performing at least five consecutive adsorption–desorption cycles under seawater conditions will help assess the retention of adsorption capacity and rejection efficiency. Complementary analytical techniques such as Fourier-transform infrared spectroscopy (FTIR), thermogravimetric analysis (TGA), and scanning electron microscopy (SEM) should be employed to detect any chemical or mechanical degradation of the polymer and membrane materials over time.

Environmental and regulatory compliance is another essential aspect. The biodegradability of the polymer should be evaluated according to OECD 301B guidelines, which require at least 60 % mineralization within 28 days. In addition, both acute (48-hour LC_{50}) and chronic ecotoxicity tests should be conducted across multiple trophic levels to assess the environmental impact of polymer residues. Identifying and tracking the major breakdown products of the polymer will be crucial for defining safe discharge limits and obtaining regulatory approval.

From an economic perspective, a comprehensive techno-economic model must be developed to compare the UF/NF–complexation approach with alternative uranium recovery methods, such as amidoxime-functionalized fibers and electrochemical extraction. This model should account for all relevant cost factors, including polymer synthesis, acid consumption, membrane replacement, energy requirements, and waste treatment. Identifying the primary cost drivers and benchmarking against the target cost of $80–100 per kilogram of uranium will be essential. Additionally, life cycle cost (LCC) modeling and life cycle assessment (LCA) studies should be conducted to quantify resource consumption, emissions, and the overall environmental footprint of the process.

Scaling up the process presents further challenges, particularly in ensuring homogeneous polymer dispersion and efficient mass transfer in large volumes ranging from 10 to 100 tons. Computational fluid dynamics (CFD) simulations and pilot-scale trials should be used to optimize mixing strategies, contact times, and the configuration of continuous feed–permeate–retentate loops. In-situ polymer recovery methods, such as thermally triggered gelation, should also be explored to enhance process efficiency.

Finally, the risk of biofouling must be thoroughly assessed. Real seawater trials should be conducted to monitor microbial colonization and biofilm formation on UF/NF membranes. Quantifying the resulting losses in flux and rejection performance will inform the development of mitigation strategies, which may include periodic backwashing, ultraviolet (UV) pretreatment, or the application of antimicrobial coatings.

By systematically addressing these multifaceted challenges, complexation-assisted UF/NF technology can progress from a promising proof-of-concept to a robust, scalable, and sustainable solution for uranium recovery from seawater. Moreover, the insights gained through this development process may also facilitate the extraction of other critical metals from high-salinity streams.

CRediT authorship contribution statement

C. Xing: Writing – review & editing, Writing – original draft, Software, Methodology, Investigation, Formal analysis, Data curation, Conceptualization. **B. Bernicot:** Methodology, Investigation, Formal analysis, Data curation, Conceptualization. **S. Monge:** Methodology. **V. Darcos:** Methodology. **G. Arrachart:** Writing – review & editing, Validation, Supervision, Resources, Project administration, Methodology, Conceptualization. **S. Pellet-Rostaing:** Writing – review & editing, Validation, Supervision, Resources, Project administration, Methodology, Funding acquisition, Conceptualization.

Funding

The authors are grateful to the China Scholarship Council (CSC) for PhD funding and DECAP project (No. ANR-18-ASTR-0001).

Declaration of competing interest

The authors declare that they have no known competing financial interests or personal relationships that could have appeared to influence the work reported in this paper.

Acknowledgments

The authors acknowledge Béatrice Baus-Lagarde, for her help regarding the ICP/OES experiments.

Appendix A. Supplementary data

Supplementary data to this article can be found online at https://doi.org/10.1016/j.desal.2025.119083.

Data availability

Data will be made available on request.

References

[1] D.S. Sholl, Seven chemical separations, Nature 532 (2016) 435–437, https://doi.org/10.1038/532435a.
[2] NEA and IAEA, Uranium: Resources, Production and Demand. https://linkinghub.elsevier.com/retrieve/pii/0301420780900501, 2020.
[3] L. Rao, Recent International R & D Activities in the Extraction of Uranium From Seawater, LBNL Paper LBNL-4034E. https://escholarship.org/uc/item/12h981cf, 2011.
[4] P. Loganathan, G. Naidu, S. Vigneswaran, Mining valuable minerals from seawater: a critical review, Environ. Sci.: Water Res. Technol. 3 (2017) 37–53, https://doi.org/10.1039/c6ew00268d.
[5] F. Endrizzi, C.J. Leggett, L. Rao, Scientific basis for efficient extraction of uranium from seawater. I: understanding the chemical speciation of uranium under seawater conditions, Ind. Eng. Chem. Res. 55 (15) (2016) 4249–4256, https://doi.org/10.1021/ACS.IECR.5B03679.
[6] U. Bardi, Extracting minerals from seawater: an energy analysis, Sustainability 2 (2010), https://doi.org/10.3390/su2040980.
[7] J. Kim, C. Tsouris, R.T. Mayes, Y. Oyola, T. Saito, C.J. Janke, S. Dai, E. Schneider, D. Sachde, Recovery of uranium from seawater: a review of current status and future research needs, Sep. Sci. Technol. 48 (2013), https://doi.org/10.1080/01496395.2012.712599.
[8] M.S. Diallo, M.R. Kotte, M. Cho, Mining critical metals and elements from seawater: opportunities and challenges, Environ. Sci. Technol. 49 (2015) 9390–9399, https://doi.org/10.1021/acs.est.5b00463.

[9] J.Y. Lee, M. Vespa, X. Gaona, K. Dardenne, J. Rothe, T. Rabung, M. Altmaier, J. I. Yun, Formation, stability and structural characterization of ternary $MgUO_2(CO_3)_3^{2-}$ and $Mg_2UO_2(CO_3)_{3(aq)}$ complexes, Radiochim. Acta 105 (2017) 171–185, https://doi.org/10.1515/ract-2016-2643.

[10] J.Y. Lee, J.I. Yun, Formation of ternary CaUO2(CO3)32− and Ca2UO2(CO3)3(aq) complexes under neutral to weakly alkaline conditions, Dalton Trans. 42 (27) (2013) 9862–9869, https://doi.org/10.1039/c3dt50863c.

[11] C.W. Abney, R.T. Mayes, T. Saito, S. Dai, Materials for the recovery of uranium from seawater, Chem. Rev. 117 (2017) 13935–14013, https://doi.org/10.1021/acs.chemrev.7b00355.

[12] H. Lindner, E. Schneider, Review of cost estimates for uranium recovery from seawater, Energy Econ. 49 (2015) 9–22, https://doi.org/10.1016/j.eneco.2015.01.016.

[13] D. Li, Z. Chen, F. Zhang, Z. Zhang, C. Chen, D. Zhang, X. Xu, Nano-tentacled interconnected channels organic gel for rapid uranium extraction from seawater, J. Hazard. Mater. 480 (2024) 135784, https://doi.org/10.1016/j.jhazmat.2024.135784.

[14] J. Gan, L. Zhang, Q. Wang, Q. Xin, Y. Xiong, E. Hu, Z. Lei, H. Wang, H. Wang, Phosphorylation improved the competitive U/V adsorption on chitosan-based adsorbent containing amidoxime for rapid uranium extraction from seawater, Int. J. Biol. Macromol. 238 (2023) 124074, https://doi.org/10.1016/j.ijbiomac.2023.124074.

[15] S.D. Alexandratos, X. Zhu, M. Florent, R. Sellin, Polymer-supported bifunctional amidoximes for the sorption of uranium from seawater, Ind. Eng. Chem. Res. 55 (2016) 4208–4216, https://doi.org/10.1021/acs.iecr.5b03742.

[16] T.S. Anirudhan, G.S. Lekshmi, F. Shainy, Synthesis and characterization of amidoxime modified chitosan/bentonite composite for the adsorptive removal and recovery of uranium from seawater, J. Colloid Interface Sci. 534 (2019) 248–261, https://doi.org/10.1016/j.jcis.2018.09.009.

[17] S. Das, W.-P. Liao, M. Flicker Byers, C. Tsouris, C.J. Janke, R.T. Mayes, E. Schneider, L.-J. Kuo, J.R. Wood, G.A. Gill, S. Dai, Alternative alkaline conditioning of amidoxime based adsorbent for uranium extraction from seawater, Ind. Eng. Chem. Res. 55 (2016) 4303–4312, https://doi.org/10.1021/acs.iecr.5b03210.

[18] J.A. Drysdale, K.O. Buesseler, Uranium adsorption behaviour of amidoximated fibers under coastal ocean conditions, Prog. Nucl. Energy 119 (2020) 103170, https://doi.org/10.1016/j.pnucene.2019.103170.

[19] J. Gao, Y. Yuan, Q. Yu, B. Yan, Y. Qian, J. Wen, C. Ma, S. Jiang, X. Wang, N. Wang, Bio-inspired antibacterial cellulose paper-poly(amidoxime) composite hydrogel for highly efficient uranium(vi) capture from seawater, Chem. Commun. 56 (2020) 3935–3938, https://doi.org/10.1039/c9cc09936k.

[20] C. Gunathilake, J. Górka, S. Dai, M. Jaroniec, Amidoxime-modified mesoporous silica for uranium adsorption under seawater conditions, J. Mater. Chem. A 3 (2015) 11650–11659, https://doi.org/10.1039/c5ta02863a.

[21] J. Kim, C. Tsouris, Y. Oyola, C.J. Janke, R.T. Mayes, S. Dai, G. Gill, L.J. Kuo, J. Wood, K.Y. Choe, E. Schneider, H. Lindner, Uptake of uranium from seawater by amidoxime-based polymeric adsorbent: field experiments, modeling, and updated economic assessment, Ind. Eng. Chem. Res. 53 (2014) 6076–6083, https://doi.org/10.1021/ie4039828.

[22] L.J. Kuo, C.J. Janke, J.R. Wood, J.E. Strivens, S. Das, Y. Oyola, R.T. Mayes, G. A. Gill, Characterization and testing of amidoxime-based adsorbent materials to extract uranium from natural seawater, Ind. Eng. Chem. Res. 55 (2015), https://doi.org/10.1021/acs.iecr.5b03267.

[23] M. Ou, W. Li, Z. Huang, X. Xu, Highly efficient extraction of uranium(VI) from seawater by polyamidoxime/polyethyleneimine sponge, Sep. Purif. Technol. 331 (2024) 125721, https://doi.org/10.1016/j.seppur.2023.125721.

[24] A.I. Wiechert, A.P. Ladshaw, L.-J. Kuo, H.-B. Pan, J. Strivens, N. Schlafer, J. R. Wood, C. Wai, G. Gill, S. Yiacoumi, C. Tsouris, Uranium recovery from seawater using amidoxime-based braided polymers synthesized from acrylic fibers, Ind. Eng. Chem. Res. 59 (2020) 13988–13996, https://doi.org/10.1021/acs.iecr.0c01573.

[25] J. Zeng, H. Zhang, Y. Sui, N. Hu, D. Ding, F. Wang, J. Xue, Y. Wang, New amidoxime-based material TMP-g-AO for uranium adsorption under seawater conditions, Ind. Eng. Chem. Res. 56 (2017) 5021–5032, https://doi.org/10.1021/acs.iecr.6b05006.

[26] X. Xu, X.J. Ding, J.X. Ao, R. Li, Z. Xing, X.Y. Liu, X.J. Guo, G.Z. Wu, H.J. Ma, X. Y. Zhao, Preparation of amidoxime-based PE/PP fibers for extraction of uranium from aqueous solution, Nucl. Sci. Tech. 30 (2019), https://doi.org/10.1007/s41365-019-0543-0.

[27] N. Tang, J. Liang, C. Niu, H. Wang, Y. Luo, W. Xing, S. Ye, C. Liang, H. Guo, J. Guo, Y. Zhang, G. Zeng, Amidoxime-based materials for uranium recovery and removal, J. Mater. Chem. A 8 (2020) 7588–7625, https://doi.org/10.1039/c9ta14082d.

[28] A. Favre-Réguillon, G. Lebuzit, J. Foos, A. Guy, A. Sorin, M. Lemaire, M. Draye, Selective rejection of dissolved uranium carbonate from seawater using cross-flow filtration technology, Sep. Sci. Technol. (2005), https://doi.org/10.1081/SS-200042529.

[29] T. Arumugham, N.J. Kaleekkal, S. Gopal, J. Nambikkattu, R. K, A.M. Aboulella, S. Ranil Wickramasinghe, F. Banat, Recent developments in porous ceramic membranes for wastewater treatment and desalination: a review, J. Environ. Manag. 293 (2021) 112925, https://doi.org/10.1016/j.jenvman.2021.112925.

[30] M. Bassyouni, M.H. Abdel-Aziz, M.Sh. Zoromba, S.M.S. Abdel-Hamid, E. Drioli, A review of polymeric nanocomposite membranes for water purification, J. Ind. Eng. Chem. 73 (2019) 19–46, https://doi.org/10.1016/j.jiec.2019.01.045.

[31] C. Liu, X. Zhao, A.F. Faria, K.Y. Deliz Quiñones, C. Zhang, Q. He, J. Ma, Y. Shen, Y. Zhi, Evaluating the efficiency of nanofiltration and reverse osmosis membrane processes for the removal of per- and polyfluoroalkyl substances from water: a critical review, Sep. Purif. Technol. 302 (2022) 122161, https://doi.org/10.1016/j.seppur.2022.122161.

[32] Z.-Y. Guo, Z.-Y. Ji, Q.-B. Chen, J. Liu, Y.-Y. Zhao, F. Li, Z.-Y. Liu, J.-S. Yuan, Prefractionation of LiCl from concentrated seawater/salt lake brines by electrodialysis with monovalent selective ion exchange membranes, J. Clean. Prod. 193 (2018) 338–350, https://doi.org/10.1016/j.jclepro.2018.05.077.

[33] J. Song, T. Huang, H. Qiu, X. Niu, X.M. Li, Y. Xie, T. He, A critical review on membrane extraction with improved stability: potential application for recycling metals from city mine, Desalination 440 (2018) 18–38, https://doi.org/10.1016/j.desal.2018.01.007.

[34] X. Zhang, W. Zhao, Y. Zhang, V. Jegatheesan, A review of resource recovery from seawater desalination brine, Rev. Environ. Sci. Biotechnol. 20 (2021) 333–361, https://doi.org/10.1007/s11157-021-09570-4.

[35] A. Taghvaie Nakhjiri, H. Sanaeepur, A. Ebadi Amooghin, M.M.A. Shirazi, Recovery of precious metals from industrial wastewater towards resource recovery and environmental sustainability: a critical review, Desalination 527 (2022) 115510, https://doi.org/10.1016/j.desal.2021.115510.

[36] F. Chitry, S. Pellet-Rostaing, C. Gozzi, M. Lemaire, Separation of lanthanides(III) by nanofiltration-complexation in aqueous medium, Sep. Sci. Technol. 36 (2001), https://doi.org/10.1081/SS-100102949.

[37] J. Borrini, G. Bernier, S. Pellet-Rostaing, A. Favre-Reguillon, M. Lemaire, Separation of lanthanides(III) by inorganic nanofiltration membranes using a water soluble complexing agent, J. Membr. Sci. 348 (2010), https://doi.org/10.1016/j.memsci.2009.10.034.

[38] F. Chitry, S. Pellet-Rostaing, A. Guy, J. Foos, M. Lemaire, Separation of americium (III) from lanthanides(III) by nanofiltration-complexation in aqueous medium, J. Radioanal. Nucl. Chem. 251 (2002), https://doi.org/10.1023/A:1015075101632.

[39] A. Favre-Réguillon, A. Sorin, S. Pellet-Rostaing, G. Bernier, M. Lemaire, Nanofiltration assisted by complexation: a promising process for the separation of trivalent long-lived minor actinides from lanthanides, Comptes Rendus Chim. 10 (2007) 994–1000, https://doi.org/10.1016/J.CRCI.2007.01.012.

[40] A. Sorin, A. Favre-Réguillon, S. Pellet-Rostaing, M. Sbaï, A. Szymczyk, P. Fievet, M. Lemaire, Rejection of Gd(III) by nanofiltration assisted by complexation on charged organic membrane: influences of pH, pressure, flux, ionic strength and temperature, J. Membr. Sci. 267 (2005), https://doi.org/10.1016/j.memsci.2005.05.022.

[41] J. Borrini, A. Favre-Reguillon, M. Lemaire, S. Gracia, G. Arrachart, G. Bernier, X. Hérès, C. Hill, S. Pellet-Rostaing, Water soluble PDCA derivatives for selective ln(III)/an(III) and am(III)/cm(III) separation, Solvent Extr. Ion Exch. 33 (2015), https://doi.org/10.1080/07366299.2014.974449.

[42] A. Favre-Réguillon, G. Lebuzit, D. Murat, J. Foos, C. Mansour, M. Draye, Selective removal of dissolved uranium in drinking water by nanofiltration, Water Res. 42 (2008), https://doi.org/10.1016/j.watres.2007.08.034.

[43] A. Favre-Reguillon, G. Lebuzit, J. Foos, A. Guy, M. Draye, M. Lemaire, Selective concentration of uranium from seawater by nanofiltration, Ind. Eng. Chem. Res. 42 (2003), https://doi.org/10.1021/ie030157a.

[44] C. Xing, B. Bernicot, G. Arrachart, S. Pellet-Rostaing, Application of ultra/nano filtration membrane in uranium rejection from fresh and salt waters, Sep. Purif. Technol. 314 (2023) 123543, https://doi.org/10.1016/j.seppur.2023.123543.

[45] J. Ramkumar, K.S. Shrimal, B. Maiti, T.S. Krishnamoorthy, Selective permeation of Cu^{2+} and UO_2^{2+} through a Nafion ionomer membrane, J. Membr. Sci. 116 (1996) 31–37, https://doi.org/10.1016/0376-7388(96)00007-5.

[46] T.M. McCleskey, D.S. Ehler, J.S. Young, D.R. Pesiri, G.D. Jarvinen, N.N. Sauer, Asymmetric membranes with modified gold films as selective gates for metal ion separations, J. Membr. Sci. 210 (2002) 273–278, https://doi.org/10.1016/S0376-7388(02)00387-3.

[47] L.A. Richards, B.S. Richards, A.I. Schäfer, Renewable energy powered membrane technology: salt and inorganic contaminant removal by nanofiltration/reverse osmosis, J. Membr. Sci. 369 (2011) 188–195, https://doi.org/10.1016/j.memsci.2010.11.069.

[48] Y.A. Boussouga, B.S. Richards, A.I. Schäfer, Renewable energy powered membrane technology: system resilience under solar irradiance fluctuations during the treatment of fluoride-rich natural waters by different nanofiltration/reverse osmosis membranes, J. Membr. Sci. 617 (2021), https://doi.org/10.1016/j.memsci.2020.118452.

[49] C. Oumar Anne, D. Trébouet, P. Jaouen, F. Quéméneur, Nanofiltration of seawater: fractionation of mono-and multi-valent cations, Desalination 140 (2001), https://doi.org/10.1016/S0011-9164(01)00355-1.

[50] S. Mimoune, F. Amrani, Experimental study of metal ions removal from aqueous solutions by complexation-ultrafiltration, J. Membr. Sci. 298 (2007) 92–98, https://doi.org/10.1016/j.memsci.2007.04.003.

[51] B.Ya. Spivakov, K. Geckeler, E. Bayer, Liquid-phase polymer-based retention — the separation of metals by ultrafiltration on polychelatogens, Nature 315 (1985) 313–315, https://doi.org/10.1038/315313a0.

[52] B.L. Rivas, E.D. Pereira, M. Palencia, J. Sánchez, Water-soluble functional polymers in conjunction with membranes to remove pollutant ions from aqueous solutions, Prog. Polym. Sci. Oxf. 36 (2011) 294–322, https://doi.org/10.1016/j.progpolymsci.2010.11.001.

[53] B.L. Rivas, S.A. Pooley, E.D. Pereira, R. Cid, M. Luna, M.A. Jara, K.E. Geckeler, Water-soluble amine and imine polymers with the ability to bind metal ions in conjunction with membrane filtration, J. Appl. Polym. Sci. 96 (2005) 222–231, https://doi.org/10.1002/app.21425.

[54] S. Verbych, M. Bryk, M. Zaichenko, Water treatment by enhanced ultrafiltration, Desalination 198 (2006) 295–302, https://doi.org/10.1016/j.desal.2005.12.029.

[55] S. Verbych, M. Bryk, A. Alpatova, G. Chornokur, Ground water treatment by enhanced ultrafiltration, Desalination 179 (2005) 237–244, https://doi.org/10.1016/j.desal.2004.11.070.

[56] R. Molinari, S. Gallo, P. Argurio, Metal ions removal from wastewater or washing water from contaminated soil by ultrafiltration-complexation, Water Res. 38 (2004) 593–600, https://doi.org/10.1016/j.watres.2003.10.024.

[57] R. Molinari, P. Argurio, T. Poerio, Ultrafiltration of polymer-metal complexes for metal ion removal from wastewaters, Macromol. Symp. 235 (2006) 206–214, https://doi.org/10.1002/masy.200650325.

[58] S. Mimoune, R.E. Belazzougui, F. Amrani, Purification of aqueous solutions of metal ions by ultrafiltration, Desalination 217 (2007) 251–259, https://doi.org/10.1016/j.desal.2007.01.016.

[59] A. Kryvoruchko, L. Yurlova, B. Kornilovich, Purification of water containing heavy metals by chelating-enhanced ultrafiltration, Desalination 144 (2002) 243–248, https://doi.org/10.1016/S0011-9164(02)00319-3.

[60] A. Sorin, S. Pellet-Rostaing, A. Favre-Reguillon, M. Lemaire, Cs^+/Na^+ separation by nanofiltration-complexation with resorcinarene, Sep. Sci. Technol. 39 (2004) 2577–2595, https://doi.org/10.1081/SS-200026721.

[61] S. Pellet-Rostaing, F. Chitry, J.A. Spitz, A. Sorin, A. Favre-Réguillon, M. Lemaire, New water-soluble calix[4]arene-bis(benzocrown-6) for caesium-sodium separation by nanofiltration-complexation, Tetrahedron 59 (2003) 10313–10324, https://doi.org/10.1016/j.tet.2003.10.051.

[62] S.-H. Lin, T.-Y. Wang, R.-S. Juang, Metal rejection by nanofiltration from diluted solutions in the presence of complexing agents, Sep. Sci. Technol. 39 (2005) 363–376, https://doi.org/10.1081/SS-120027563.

[63] G. Crini, N. Morin-Crini, N. Fatin-Rouge, S. Déon, P. Fievet, Metal removal from aqueous media by polymer-assisted ultrafiltration with chitosan, Arab. J. Chem. 10 (2017) S3826–S3839, https://doi.org/10.1016/j.arabjc.2014.05.020.

[64] B.L. Rivas, S. Hube, J. Sánchez, E. Pereira, Chelating water-soluble polymers associated with ultrafiltration membranes for metal ion removal, Polym. Bull. 69 (2012) 881–898, https://doi.org/10.1007/s00289-012-0785-z.

[65] K. Trivunac, S. Stevanovic, Removal of heavy metal ions from water by complexation-assisted ultrafiltration, Chemosphere 64 (2006) 486–491, https://doi.org/10.1016/j.chemosphere.2005.11.073.

[66] P.G. Bansod, D. Bhutada, S. Barkade, S. Kodape, Enhancement of separation efficiency for nano filtration membrane using water-soluble polymer, Int. J. Recent Technol. Eng. 8 (2019) 1470–1474, https://doi.org/10.35940/ijrte.B2112.078219.

[67] L. Yurlova, A. Kryvoruchko, B. Kornilovich, Removal of Ni(II) ions from wastewater by micellar-enhanced ultrafiltration, Desalination 144 (2002) 255–260, https://doi.org/10.1016/S0011-9164(02)00321-1.

[68] B.L. Rivas, S.A. Pooley, E. Pereira, E. Montoya, R. Cid, K.E. Geckeler, Water-soluble polymer materials as complexing reagents for the separation of metal ions using membrane filtration, Polym. Adv. Technol. 17 (2006) 865–871, https://doi.org/10.1002/pat.791.

[69] K.E. Geckeler, K. Volchek, Removal of hazardous substances from water using ultrafiltration in conjunction with soluble polymers, Environ. Sci. Technol. 30 (1996) 726–734, https://doi.org/10.1021/es950326l.

[70] A.B. Yusov, V.I. Mishkevich, A.M. Fedoseev, M.S. Grigor'Ev, Complexation of An (VI) (An = U, Np, Pu, Am) with 2,6-pyridinedicarboxylic acid in aqueous solutions. Synthesis and structures of new crystalline compounds of U(VI), np(VI), and Pu(VI), Radiochemistry 55 (2013) 269–278, https://doi.org/10.1134/S1066362213030053.

[71] M.A. Brown, A. Paulenova, A.V. Gelis, Aqueous complexation of thorium(IV), uranium(IV), neptunium(IV), plutonium(III/IV), and cerium(III/IV) with DTPA, Inorg. Chem. 51 (2012) 7741–7748, https://doi.org/10.1021/ic300757k.

[72] A. Garai, P. Delangle, Recent advances in uranyl binding in proteins thanks to biomimetic peptides, J. Inorg. Biochem. 203 (2020) 110936, https://doi.org/10.1016/j.jinorgbio.2019.110936.

[73] A.P. Kryvoruchko, L.Y. Yurlova, I.D. Atamanenko, B.Y. Kornilovich, Ultrafiltration removal of U(VI) from contaminated water, Desalination 162 (2004) 229–236, https://doi.org/10.1016/S0011-9164(04)00046-3.

[74] P. Reiller, Dual use of micellar-enhanced ultrafiltration and time-resolved laser-induced spectrofluorimetry for the study of uranyl exchange at the surface of alkylsulfate micelles, J. Colloid Interface Sci. 163 (1994) 81–86, https://doi.org/10.1006/jcis.1994.1082.

[75] M. Huang, L. Xie, Y. Wang, X. Feng, J. Gao, Z. Lou, Y. Xiong, Efficient and selective capture of uranium by polyethyleneimine-modified chitosan composite microspheres from radioactive nuclear waste, Environ. Pollut. 316 (2023) 120550, https://doi.org/10.1016/j.envpol.2022.120550.

[76] Y.-C. Yue, M.-H. Li, H.-B. Wang, B.-L. Zhang, W. He, The toxicological mechanisms and detoxification of depleted uranium exposure, Environ. Health Prev. Med. 23 (2018) 18, https://doi.org/10.1186/s12199-018-0706-3.

[77] J.D. Roach, J.H. Zapien, Inorganic ligand-modified, colloid-enhanced ultrafiltration: a novel method for removing uranium from aqueous solution, Water Res. 43 (2009) 4751–4759, https://doi.org/10.1016/j.watres.2009.08.007.

[78] H. Shojaei, A. Keshtkar, M. Moosavian, M.G. Torkabad, Modeling uranium (II) removal from aqueous solution by micellar enhanced ultrafiltration using response surface methodology, Groundw. Sustain. Dev. 15 (2021) 100660, https://doi.org/10.1016/j.gsd.2021.100660.

[79] M. Ahmad, J. Ren, Y. Zhang, H. Kou, M. Naik, Q. Zhang, B. Zhang, Simple and facile preparation of tunable chitosan tubular nanocomposite microspheres for fast uranium(VI) removal from seawater, Chem. Eng. J. 427 (2022) 130934, https://doi.org/10.1016/j.cej.2021.130934.

[80] Vincent Darcos, Loona Ferrie, Carlos Arrambide Cruz, Gabriele Vecchio, Nicolas Dacheux, Stéphane Pellet-Rostaing, Benedicte Prelot, Sophie Monge, Tailored bisphosphonate functionalized polyacrylamide for enhanced actinide recovery, in: , 2025. Submitted.

[81] R. Turgis, A. Leydier, G. Arrachart, F. Burdet, S. Dourdain, G. Bernier, M. Miguirditchian, S. Pellet-Rostaing, Uranium extraction from phosphoric acid using bifunctional amido-phosphonic acid ligands, Solvent Extr. Ion Exch. 32 (2014) 478–491, https://doi.org/10.1080/07366299.2014.898435.

[82] P. Yang, Q. Liu, J. Liu, R. Chen, R. Li, X. Bai, J. Wang, Highly efficient immobilization of uranium(VI) from aqueous solution by phosphonate-functionalized dendritic fibrous nanosilica (DFNS), J. Hazard. Mater. 363 (2019) 248–257, https://doi.org/10.1016/j.jhazmat.2018.09.062.

[83] W. Yang, T.G. Parker, Z.-M. Sun, Structural chemistry of uranium phosphonates, Coord. Chem. Rev. 303 (2015) 86–109, https://doi.org/10.1016/j.ccr.2015.05.010.

[84] P. Singhal, B.G. Vats, A. Yadav, V. Pulhani, Efficient extraction of uranium from environmental samples using phosphoramide functionalized magnetic nanoparticles: understanding adsorption and binding mechanisms, J. Hazard. Mater. 384 (2020) 121353, https://doi.org/10.1016/j.jhazmat.2019.121353.

[85] V. Beaugeard, J. Muller, A. Graillot, X. Ding, J.J. Robin, S. Monge, Acidic polymeric sorbents for the removal of metallic pollution in water: a review, React. Funct. Polym. 152 (2020) 104599, https://doi.org/10.1016/j.reactfunctpolym.2020.104599.

[86] D. Prabhakaran, M.S. Subramanian, Extraction of U(VI), Th(IV), and La(III) from acidic streams and geological samples using AXAD-16-POPDE polymer, Anal. Bioanal. Chem. 380 (2004) 578–585, https://doi.org/10.1007/s00216-004-2729-4.

[87] T. Vasudevan, A.K. Pandey, S. Das, P.K. Pujari, Poly(ethylene glycol methacrylate phosphate-co-2-acrylamido-2-methyl-1-propane sulfonate) pore-filled substrates for heavy metal ions sorption, Chem. Eng. J. 236 (2014) 9–16, https://doi.org/10.1016/j.cej.2013.09.064.

[88] A. Graillot, D. Bouyer, S. Monge, J.-J. Robin, C. Faur, Removal of nickel ions from aqueous solution by low energy-consuming sorption process involving thermosensitive copolymers with phosphonic acid groups, J. Hazard. Mater. 244–245 (2013) 507–515, https://doi.org/10.1016/j.jhazmat.2012.10.031.

[89] A. Graillot, C. Cojocariu, D. Bouyer, S. Monge, S. Mauchauffe, J.-J. Robin, C. Faur, Thermosensitive polymer enhanced filtration (TEF) process: an innovative process for heavy metals removal and recovery from industrial wastewaters, Sep. Purif. Technol. 141 (2015) 17–24, https://doi.org/10.1016/j.seppur.2014.11.023.

[90] M. Sawicki, J.M. Siaugue, C. Jacopin, C. Moulin, T. Bailly, R. Burgada, S. Meunier, P. Baret, J.L. Pierre, F. Taran, Discovery of powerful uranyl ligands from efficient synthesis and screening, Chem. Eur. J. 11 (2005) 3689–3697, https://doi.org/10.1002/chem.200401056.

[91] A.E.V. Gorden, J. Xu, K.N. Raymond, P. Durbin, Rational design of sequestering agents for plutonium and other actinides, Chem. Rev. 103 (2003) 4207–4282, https://doi.org/10.1021/cr990114x.

[92] K.L. Nash, Stability and stoichiometry of uranyl phosphonate coordination compounds in acidic aqueous, Solutions 4 (1993) 147–154, https://doi.org/10.1524/ract.1993.61.34.147.

[93] S.K. Verma, R.P. Agarwal, Stability and polymerization of uranyl-catechol chelates, J. Für Prakt. Chem. 38 (1968) 280–288, https://doi.org/10.1002/prac.19680380507.

[94] A.K. Alwan, P.A. Williams, The aqueous chemistry of uranium minerals. Part 2. Minerals of the liebigite group, Mineral. Mag. 43 (1980) 665–667, https://doi.org/10.1180/minmag.1980.043.329.17.

[95] D. Gomes Rodrigues, S. Monge, S. Pellet-Rostaing, N. Dacheux, D. Bouyer, C. Faur, Sorption properties of carbamoylmethylphosphonated-based polymer combining both sorption and thermosensitive properties: new valuable hydrosoluble materials for rare earth elements sorption, Chem. Eng. J. 355 (2019) 871–880, https://doi.org/10.1016/j.cej.2018.08.190.

[96] K. McCann, B.J. Mincher, N.C. Schmitt, J.C. Braley, Hexavalent actinide extraction using N,N-dialkyl amides, Ind. Eng. Chem. Res. 56 (2017) 6515–6519, https://doi.org/10.1021/acs.iecr.7b01181.

[97] O. Clement, B.M. Rapko, B.P. Hay, Structural aspects of metal–amide complexes, Coord. Chem. Rev. 170 (1998) 203–243, https://doi.org/10.1016/S0010-8545(98)00066-6.

[98] K.L. Nash, F-element complexation by diphosphonate ligands, J. Alloys Compd. 249 (1997) 33–40, https://doi.org/10.1016/S0925-8388(96)02520-0.

[99] C.M. Sevrain, M. Berchel, H. Couthon, P.-A. Jaffrès, Phosphonic acid: preparation and applications, Beilstein J. Org. Chem. 13 (2017) 2186–2213, https://doi.org/10.3762/bjoc.13.219.

[100] J. Ke, H. Dou, X. Zhang, D.S. Uhagaze, X. Ding, Y. Dong, Determination of pKa values of alendronate sodium in aqueous solution by piecewise linear regression based on acid-base potentiometric titration, J. Pharm. Anal. 6 (2016) 404–409, https://doi.org/10.1016/j.jpha.2016.07.001.

[101] Q. Lin, Q. Li, C. Batchelor-McAuley, R.G. Compton, Two-electron, two-proton oxidation of catechol: kinetics and apparent catalysis, J. Phys. Chem. C 119 (2015) 1489–1495, https://doi.org/10.1021/jp511414b.

[102] R.S. Oguike, Corrosion studies on stainless steel (FE6956) in hydrochloric acid solution, Adv. Mater. Phys. Chem. 4 (2014) 153–163, https://doi.org/10.4236/ampc.2014.48018.

[103] H. Chen, J. Li, Y. Ding, G. Zhang, Q. Zhang, C. Wu, Folding and unfolding of individual PNIPAM-g-PEO copolymer chains in dilute aqueous solutions, Macromolecules 38 (2005) 4403–4408, https://doi.org/10.1021/ma050222n.

[104] S. Moelbert, B. Normand, P. De Los Rios, Kosmotropes and chaotropes: modelling preferential exclusion, binding and aggregate stability, Biophys. Chem. 112 (2004) 45–57, https://doi.org/10.1016/j.bpc.2004.06.012.
[105] N.J. Bridges, K.E. Gutowski, R.D. Rogers, Investigation of aqueous biphasic systems formed from solutions of chaotropic salts with kosmotropic salts (salt–salt ABS), Green Chem. 9 (2007) 177–183, https://doi.org/10.1039/b611628k.
[106] Y. Zhang, S. Furyk, L.B. Sagle, Y. Cho, D.E. Bergbreiter, P.S. Cremer, Effects of Hofmeister anions on the LCST of PNIPAM as a function of molecular weight, J. Phys. Chem. C 111 (2007) 8916–8924, https://doi.org/10.1021/jp0690603.
[107] J. Zhang, P. Ju, C. Wang, Y. Dun, X. Zhao, Y. Zuo, Y. Tang, Corrosion behaviour of 316L stainless steel in hot dilute sulphuric acid solution with sulphate and NaCl, Prot. Met. Phys. Chem. Surf. 55 (2019) 148–156, https://doi.org/10.1134/S207020511901026X.
[108] E. Otero, A. Pardo, E. Sáenz, M.V. Utrilla, P. Hierro, A study of the influence of nitric acid concentration on the corrosion resistance of sintered austenitic stainless steel, Corros. Sci. 38 (1996) 1485–1493, https://doi.org/10.1016/0010-938X(96)00039-X.
[109] M. Kazazi, M. Haghighi, D. Yarali, M.H. Zaynolabedini, Improving corrosion resistance of 316L austenitic stainless steel using ZrO2 sol-gel coating in nitric acid solution, J. Mater. Eng. Perform. 27 (2018) 1093–1102, https://doi.org/10.1007/s11665-018-3202-4.